Biomimetic sonar design and the investigation of the role of peripheral dynamics for target classification in bat biosonar

Joseph V. Sutlive

Dissertation submitted to the Faculty of the
Virginia Polytechnic Institute and State University
in partial fulfillment of the requirements for the degree of

Doctor of Philosophy
in
Translational Biology, Medicine, and Health

Rolf Müller, Chair
Stephen LaConte
Alexander Leonessa
Ignacio Moore

September 24, 2020
Blacksburg, Virginia

Keywords: Bats, Bioinspiration, Biomimetics, Soft Robotics

Biomimetic sonar design and the investigation of the role of peripheral dynamics for target classification in bat biosonar

Joseph V. Sutlive

(ABSTRACT)

The biosonar system of bats has many unique adaptations which allow for navigation in extremely cluttered environments. One such adaptation is the rapid motion of the pinna and noseleaf observed in certain families of old-world bats (Rhinolophidae and Hipposiderae). Little is known about the physical properties about this adaptation affects emitted pulses or incoming echoes. To explore the physical properties of biosonar systems utilizing dynamic peripheries, biomimetic sonar systems have been devised, which can be used to simulate the structural characteristics of the pinna and noseleaf geometry as well as the motor characteristics. Using this method, it was determined that the changing conformations of the biomimetic baffles were responsible for time-variant signatures in echoes. These signatures could be seen in echoes from a variety of both simple and complex target shapes. Then to further the capabilities of the device, an improved actuation system was devised using pneumatic actuation. This allowed for the baffles to make several unique motions as opposed to being restricted to one previously. It was also shown that the distinct motion profiles of the system led to distinct differences in the received acoustic signal. The features encoded by this system could lead to improvements in the development of improved sensing of smaller autonomous systems.

GRANT INFORMATION

This work was supported by grants from the Office of Naval Research (ONR) and the Naval Engineering Education Consortium (NEEC). Additional support was provided by an East Asia and Pacific Summer Institutes (EAPSI) fellowship from the National Science Foundation (NSF).

Biomimetic sonar design and the investigation of the role of peripheral dynamics for target classification in bat biosonar

Joseph V. Sutlive

(GENERAL AUDIENCE ABSTRACT)

Bats are known for using echolocation in addition to sight for hunting and navigating at night. The capabilities of bats and their "sonar" systems vary widely, as each species has evolved to survive in its specific environment. Certain species of bats indigenous to Eurasia are observed to perform complex motions of the outer ear and noseleaf (a ridged structure which sits atop the nostrils and acts like a "megaphone" of sorts). These bats are noted to be able to live in particularly cluttered environments and could be a particularly useful model organism for improving sonar. This is because since they are able to acquire detailed information about its surroundings with only their nostrils and ears, are able to outperform complicated man-made devices with thousands more sensing elements. To be able to better understand how a fast-moving ear and noseleaf can improve the sonar capabilities of bats, robots which mimic these bats have been devised, with the main purpose being to replicate the sensing elements of the bat. There have been significant changes made to the robotic sonar head in order to allow for us to expand the capabilities of our research. Using CT-scans as reference, the design of the baffles was redesigned to become more realistic and to have more features observed in the bats. A new method was designed in order to move the "ears" and "noseleaf" of the robot, using pneumatic actuators, which allowed for better control of the system. Finally, prototype sensors were developed to aid in the development of a motion feedback system to ensure a stable system. The robotic sonar has been used in several experiments to study the effects of a fast-moving, flexible anatomy on the physical properties of echoes. This is first illustrated by studying the echoes from various targets with changes in ear and noseleaf shape. Additionally, with the use of the improved actuation system, it was shown

that different motion profiles lead to different responses. The continued development of this system and the changes to the signals explored provide new opportunities for furthering the fields of adaptive sensing as they apply to robots and other platforms. Being able to use a few "smart" sensors will help reduce the size, power, and weight costs of traditional sensing designs and allow for more robust and efficient technology to be produced.

Acknowledgments

I would like to thank my advisor, Dr. Rolf Müller for providing me the opportunity and support to conduct this research, as well as the advice he has given me on all of my projects. Additionally, I would like to thank my committee members, Dr. Stephen LaConte, Dr. Alexander Leonessa, and Dr. Ignacio Moore for their additional support of my project and their insight. I would like to thank the directors of the graduate program in Translational Biology, Medicine, and Health, Dr. Steven Poelzing and Dr. Michelle Theus for their additional support as well. Additionally, I would like to thank all my labmates for their support and advice. I have had the privilege of being able to mentor many undergraduate students while at Virginia Tech, and thank them all for the time and effort they have devoted to the project. In particular I would like to thank Nathan Cox, Shubham Dawda, Sanmeel Lagad, Lucas Mun, Agoshpreet Singh, and Brandon Walker.I would finally like to thank my parents, Dr. Vinson Sutlive and Ann Sutlive, along with my brother, Joshua Sutlive for their love and support throughout my time here.

Contents

List of Figures

List of Tables

Chapter 1

Introduction

Sonar is a method in which sound can be used to navigate, and is either passive, in which there are no sound sources on the device, or active, wherein the device sends out a signal and listens to echoes [111]. Sonar has been used for many years to address challenges regarding navigation, oceanography, and study of marine mammals [30] Modern sonar design paradigms unfortunately have performance limitations which make their use in small or miniaturized systems, such as robots, quite difficult [66, 102]. These limitations are largely related to the amount of receivers needed in order to obtain a fine enough angular resolution; needed particularly for direction finding and classification [12, 46]. Figure 1.1 indicates the relationship between array length and angular resolution, indicating the physical limitations of conventional sonar design [1, 6] that bats are able to overcome [22, 93].

Modern robotic devices need accurate and efficient sensing devices in order to operate and navigate complex environments. Examples of this could include environments the system has not encountered before, in which case the device would have to adapt to its surroundings [16] or those which contain a large amount of clutter, where the system would need to be able to navigate and find objects where there are many possible distractors. Among the grand challenges in robotics is the goal of improving the performance of robots and their ability to achieve autonomous mobility across many environments and conditions [116].

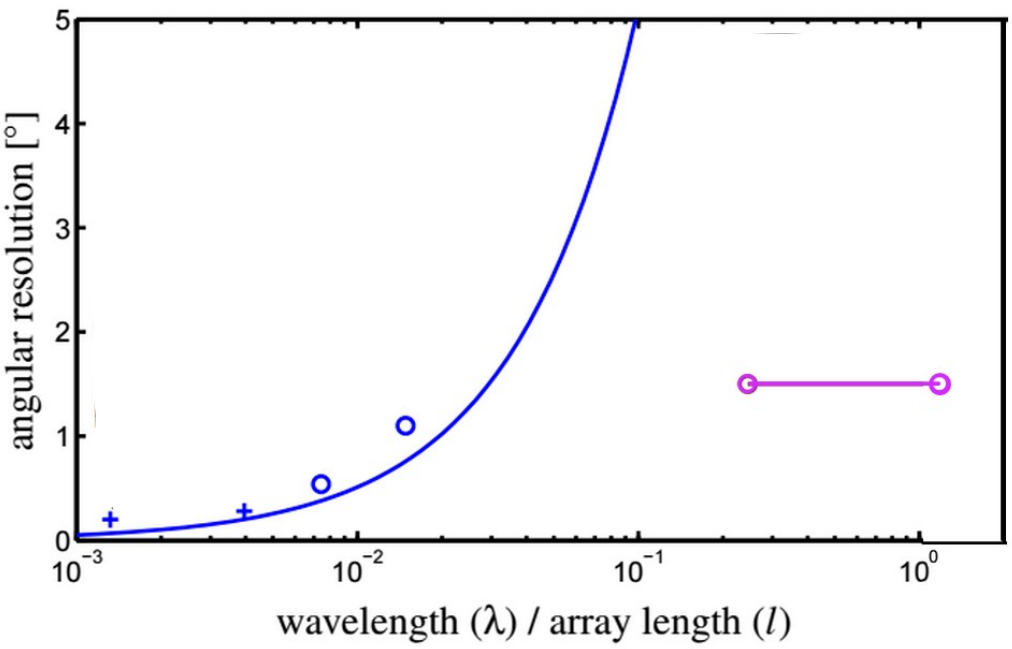

Figure 1.1: **Physical limitations of sonar as it realtes to angular resolution as a function of wavelength/ array length.**While manmade sonar(blue +/o [1, 6]) is limited by its array length, bats(purple o [22, 93]) are able to overcome these limitations by using additional principles than conventional beamforming.

1.1 Bats and Sonar

Bats are able to accomplish many of the tasks that are challenges for sonar engineers today with limited emitters and receivers (i.e. 2 nostrils/1 mouth and 2 ears). As there are 1200 known species of bats scattered across every continent (with exception of Antarctica) [115], there is quite a lot of biodiversity within the pinna and noseleaf shapes of bats [56]. This is due to the principles of adaptive radiation seen when species diverge to occupy different ecological niches [97]. Many bats have been shown to be able to hunt and forage in very cluttered environments relying primarily on echolocation as a means of sensing.

Certain families of bats (*Rhinolophidae*, *Hipposiderae*) are observed to have anatomically unique pinnae and noseleaves (a furrow-like structure that sits atop the nostrils) which allow

them to move rapidly during echolocation, within a timescale of 200 ms [33, 39, 125]. There are approximately 20 different muscles on the outer ear structures and eight in the noseleaf which allow for this to happen [87]. It is known that the acoustic effects resulting from complex geometry of the outer ear of mammals encodes spatial information from sound [53]; the geometries of the outer ear and noseleaf in these bats are quite complex, containing detailed furrows or ridges [8, 56]. which can aid in the formation of complex beampatterns [18, 64]. The pinna motion can be described as being either rigid, where the entire ear structure rotates with respect to the head [79, 121], or non-rigid, where the ear structure deforms without necessarily changing the overall structure's rotation on the head [121].

Doppler shifts have been described as changes in frequency of a wave resulting in the changing position of the observer relative to the source [26]. It has been shown that Doppler shifts play a critical role in cortical auditory processing in bats that utilize Doppler shift compensation, with a large portion of cortex devoted to what is called the Doppler-Shift Constant Frequency (DSCF) region of the auditory cortex with finely tuned elements [98, 113]. In the context of bats, Doppler shifts can originate from a variety of sources. Bats compensate for Doppler shifts resulting from their own flight [89] as well as listen to the wingbeat-frequencies from potential prey [110]. Recently it has been shown Doppler shifts can be caused by the rapid motion of the pinna of horseshoe bats [119]. It is believed this adaptation allows for these bats to be able to navigate in dense foliage [95] and explore unique environments [78].

1.2 Soft Robotics

Soft robotics is used to describe robotic designs using flexible, or "soft" materials [105], such as silicone or rubber. These designs also typically use non-rigid methods of actuation as opposed to more conventional mechanical designs using rigid components such as gears,

rods, and levers. This logically leads to a variety of novel manufacturing methods used to develop soft robots, including silicone molding [57], embedding compliant materials [20], and additive manufacturing [20, 106].There are many possible applications for the designs created by soft robots, including surgical robots [82], wearable technology [74, 76]. Due to the "soft" characteristics of this field, many biomimetic designs, in particular robot designs, use soft robotics. Examples include those of biomimetic fish [83], octopi [114], and insects [43, 90, 118].

Movement in many species has been able to be replicated using soft robotic techniques [114]. Soft robotics has also been used to explore perception-action loops, where a gradient of perceived stimuli can lead likewise to a spectrum of different possible actions [103]. With the techniques using soft robotics becoming increasingly more powerful and biomimetics providing a unique framework to develop unique engineering paradigms [13, 109], a soft-robotic representation of the fast-moving acoustic peripheries of horseshoe bats allows for a unique perspective in the field of acoustic sensing.

1.3 Biomimetic Sonar Head

Biomimetics provides a framework by which to learn about biological systems as well as adapt biological adaptations to engineered systems by developing materials, devices, and processes inspired by those that have evolved in nature [13, 109]. Biomimetic systems vary widely in animals that are modeled, design paradigms, and final application [49, 90].Emulating the mechanisms by which bats echolocate using a biomimetic design paradigm could provide insight into mechanisms for improved acoustic sensing [67]. Many prototype designs have shown the ability for bat-like sonar systems to be able to better classify objects [81], localize sound sources [120], and better discern speech patterns within noise [36, 41]. The biomimetic

sonar head has been used as a tool to gain a broader understanding of the physical properties of the biosonar system of horseshoe bats and round-leaf bats [17, 73, 117]. While there are biomimetic sonar heads designed which use a traditional beamforming approach [2], our approach was to instead focus on using only the individual biomimetic ears and noseleaf as the acoustic elements. ThereThere have been four versions of the sonar which have been used for research, with a fifth version soon to be completed (see figure 1.2). The earlier versions of the sonar head had very limited ear and noseleaf motion, with only a single degree of freedom in the ear motion and two in the noseleaf motion. Additionally, the mechanical design of the actuation system limits the ability to move the ears at variable speeds. The first design featured rubber pinnae and a deformable noseleaf structure, which was the only dynamic component. The dynamic noseleaf consisted of two flat surfaces, which could be moved in and out together. [73]. The second iteration of this design used a more detailed noseleaf, using a rubber base and some 3d printed features [17, 32]. The third version featured a more complete system, using a silicone noseleaf with a larger waveguide system in the back to increase the emitted sound level, and updated the motor systems from DC motors to stepper motors, which were smaller and allowed for a reduction in size of the system. During this time, silicone ears were molded and characterized as well.

1.4 Chapter Outline

Chapter 1 - Introduction

Chapter 2 - Shows the presence of dynamic signatures within the echoes of different targets created by an altering of the conformation state of the biomimetic pinna and noseleaf

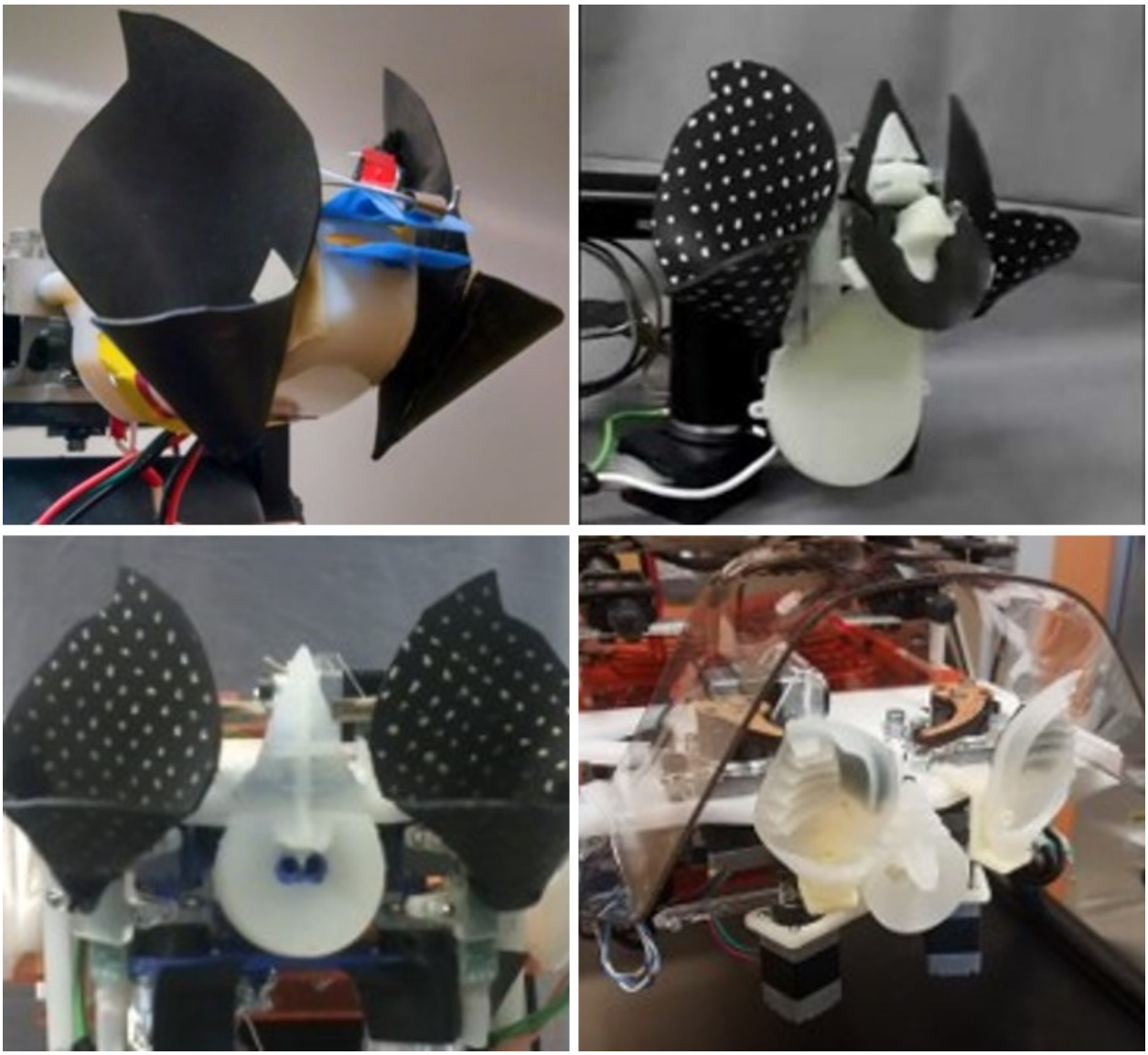

Figure 1.2: **Previous versions of the sonar head:** Clockwise, from top left: Sonar head version 1, finished February 2015; Sonar head version 2, finished April 2015;, Sonar head version 4, finished September 2018; Sonar head version 3, finished August 2016 . Sonar head version 5, currently in progress, is shown later.

Chapter 3 - Introduces a novel actuation system for a biomimetic sonar head and demonstrates the acoustic effects of different motions created by this system. Also introduces a prototype sensor system

Chapter 4 - Discussion/ conclusions

Appendix 1 - Detailed design description of the fourth model of the dynamic sonar head

Appendix 2 - Detailed design description of the fifth model of the dynamic sonar head, currently in progress

Chapter 2

Dynamic Echo Signatures Created by a Biomimetic Sonar Head

2.1 Executive Summary

Certain bat species (e.g., horseshoe bats, family Rhinolophidae) are known for conspicuous deformations of the emission baffles (noseleaves) and reception baffles (ears). Previously reported numerical studies and experiments with biomimetic reproductions of these baffles have shown that such deformations can result in time-variant emitter/receiver characteristics. However, it has not been investigated whether these time-variant characteristics could also manifest themselves in likewise time-variant properties in echoes from targets of varying complexity. To investigate this question, a biomimetic sonar head complete with deformable emission and reception baffles has been used to ensonify targets with different simple geometries (sphere, cylinder, and cube) as well as random, more natural target geometries (artificial plants) from distances of about 1 meter. Time-variant echo signatures were found in all these cases, i.e., irrespective of target complexity and whether the time-variance was injected into the emission, the reception, or into both. This demonstrates that although the time-variant emission/reception characteristics had been previously measured only under

careful conditions, they are capable of impacting real-world echoes. Even targets with distributed clouds of scattering facets did not obscure the effects of the changing conformation states. Hence these changes in ear position created by baffle deformations could serve the animals or man-made sonar systems that mimic them to encode additional echo information through time-variant echo signatures.

2.2 Introduction

Many bat species have uniquely capable biosonar systems that act as the primary source of sensory information to enable navigation in complex environments such as dense vegetation [15, 29, 69, 70]. Based solely on streams of brief, ultrasonic echoes as the only sensory link between the animals and the structures in their environments, certain bat species are able to navigate narrow passage ways in foliage [88, 95] and find their prey among numerous distracting targets [35, 70]. At present, a substantial performance gap remains between the biosonar-based capabilities of bats hunting in vegetation and the capabilities of engineered sonar [102] - as well as other technical sensing modalities [86].

The reasons for the performance gap between bat biosonar and its man-made peers have yet to be determined conclusively, but some unique features in the biosonar systems of two bat families, horseshoe bats (Rhinolophidae, 70 species, [23]) and Old World leaf-nosed bats (Hipposideridae, 74 species, [94]) could offer clues. Bats belonging to these two families have sophisticated biosonar systems that are known to rely on various dynamic mechanisms, for example, Doppler shifts induced by the wing motion of an insect prey are used to identify it in vegetation [52, 61]. Furthermore, there is a conspicuous dynamics in the periphery of these biosonar systems where baffle structures on the emission and reception side change shape as ultrasonic pulses are emitted and echoes received. On the emission side, rhinolophid

and hipposiderid bats both emit their ultrasonic pulses through nostrils that are surrounded by noseleaves, i.e., "megaphone"-like baffles. It has been shown that the unique shapes of the noseleaf baffles of CF-FM bats leads to more complex beampatterns [62]. These noseleaves change their shapes during pulse emission [28, 38] through muscular actuation [34]. Recently, a similar dynamics has been described in a New World leaf-nosed bat (*Phyllostomus discolor*, [54]). Likewise, the outer ears (pinnae) that receive the ultrasonic echoes have been shown to be in motion during echo reception [33, 119], actuated by a musculature that is even more intricate than that of the noseleaves [87].

Evidence that these changes in the noseleaf and pinna shapes have an impact on the acoustic characteristics of ultrasound emission and reception has come from numerical predictions [8, 33, 38] as well as from biomimetic systems, i.e., robotic sonar heads with actuated flexible baffles [17, 32, 58, 73, 117]. All these studies have suggested that noseleaf and pinna motion impart time-variant effects on the emitted pulses and the received echoes respectively.

However, all prior work, whether computational or physical, has been limited to estimating acoustic characterization for the emission or reception side in isolation, e.g., in the form of a time-variant beampattern (emission or reception gain as function of direction, frequency, and time). When characterizing a biomimetic ultrasonic emission system, for example, a microphone is typically placed at a short distance away from the emitter (typically 1m) which is then rotated to measure its properties from different directions [117]. The same approach is taken for characterizing reception, only that the microphone is replaced with an ultrasonic loudspeaker [17].

It has been shown that even relatively simple sonar targets typically have multiple places of echo formation [31] and this is even more true for natural targets that often have a high degree of geometrical complexity [59, 65]. Hence, there is no guarantee that time-variant effects measured with simple targets, under carefully controlled conditions, and with highly

favorable signal-to-noise ratios are of practical importance to the operation of complete sonar systems in the real world. Operation of an active sonar system includes propagation of the pulse from the emitter to a reflecting target and of the echo back to the receiver. This means substantial attenuation of the signal due to propagation losses (spreading losses and absorption, [72, 104]) and – as is often the case – low target strength (reflectivity, [72, 108]). Furthermore, the target will typically transform the temporal and spectral composition of the signal thoroughly. All these effects could reduce the visibility of time-variant properties introduced by the bats' biosonar system – potentially to an extent where they are no longer useful. This scenario is of particular concern for complex, extended targets that are frequently found in natural environments, e.g., foliages. The extended nature of a target consisting of many reflecting facets (e.g., leaves in a foliage [59, 65, 88]) distributed over a considerable volume could result in a cacophony of different time-variant signatures that may not be discernible in the result of superimposition that forms the entire echo.

In order to answer the question whether time-variant signatures like the ones created by the changing pinna and noseleaf conformations of bats can be found in the echoes received by an active sonar system, we have used a biomimetic sonar head inspired by horseshoe bats [17, 18] to ensonify targets and record the echoes returned from them with the model pinnae and noseleaf bent in different conformations. We have used targets with different simple geometries as well as natural targets (foliages) to investigate whether the geometrical complexity of the target affects the expression of time-variant properties in the echoes.

2.3 Methods

2.3.1 Sonar Head Setup

The experiments were performed using a biomimetic sonar head, modeled after the greater horseshoe bat (*Rhinolophus ferrumequinum*, Figure 2.1). The acoustic elements of the sonar head consisted of a single emitter and two receivers, each with a biomimetic baffle surrounding it. The emitter structure was designed to mimic the noseleaf and nasal emission system of horseshoe bats. The "nostrils", i.e., the outlets for the ultrasound, on this noseleaf were approximately three millimeters in diameter. Two electrostatic ultrasonic transducers (600 series, diameter 38.4 mm, SensComp, Livonia, Michigan, United States) with a -6 dB bandwidth from approximately 45 to 75 kHz and a maximum response at 55 kHz were used to generate the ultrasound. One transducer each was connected to the nostrils in the noseleaf via a conical waveguide approximately 7.6 cm in length.

The sonar head had two receivers; silicon baffles designed to mimic the outer ears of the bats, with a MEMS microphone (Monomic, Dodotronic, Rome, Italy) placed within an "ear canal" located near the base of each baffle as informed by pre-existing meshes created from CT scans of the pinnae of *R. ferrumequinum*[117]. The transducer was positioned approximately 2-3 mm behind the "ear canal" opening, facing outward towards the environment. For the experiments reported here, only one ear, the right ear, was used to collect echo data. The ear and its microphone holder were oriented at a 30° angle with respect to the aperture normal of the emitter. This was done to maintain as close a similarity as possible with regard to the positioning of the "anatomical" acoustic elements.

The shape designs for the silicone baffles were created using mesh software (Maya, Autodesk Corporation, San Rafael, California, United States) and 3d printed with polylactic acid

(PLA). The resulting model was cast in silicone (Dragonskin 30 and Eco-flex 00-30, Smooth-on, Macungie, Pennsylvania, United States). The ears were made of the stiffer of the two materials used (Dragonskin 30, with a Shore hardness of 30A; Eco-Flex 30 has a Shore hardness of 00-30).

A set of five stepper motors (PKP Series, Oriental Motor, Japan) was used to change the shapes of the baffles. The motors were driven using a microcontroller (Arduino MEGA, Arduino, Ivrea, Italy) and a dedicated driver (Easy Driver, Sparkfun, Niwot, Colorado, United States). Three motors were used to actuate the noseleaf baffle at positions on the lancet and the anterior leaf, and one motor each was used to actuate the two pinnae (Figure 2.2). In these experiments, the motors did not actively move the pinnae during individual echo measurements, but instead the motors' holding torque was used to keep the baffles in different shape configurations. The sonar head's sensor components were controlled via a data acquisition system (PXIe-6356, National Instruments, Austin, Texas, United States). Using this system, the microphone output was sampled at 500 kHz per channel at 16 bit resolution (total harmonic distortion -80 dB full scale).

2.3.2 Experimental Setup

Experiments were conducted in a similar fashion to those conducted in previous studies using biomimetic sonars [17, 64]. The sonar head was placed on a pan-tilt unit (D-28, FLIR, Wilsonville, Oregon, United States) to allow for scanning across a wide azimuth range. The targets with simple geometries were made from Styrofoam, the artificial foliages were made from plastics and/or cloth fibers. All targets were positioned one meter downrange of the sonar head in an aluminum frame padded with anechoic foam. The frame consisted of two towers 1.2 m×1.2 m×2.3 m each in size that were positioned 3 m apart. The target was hung

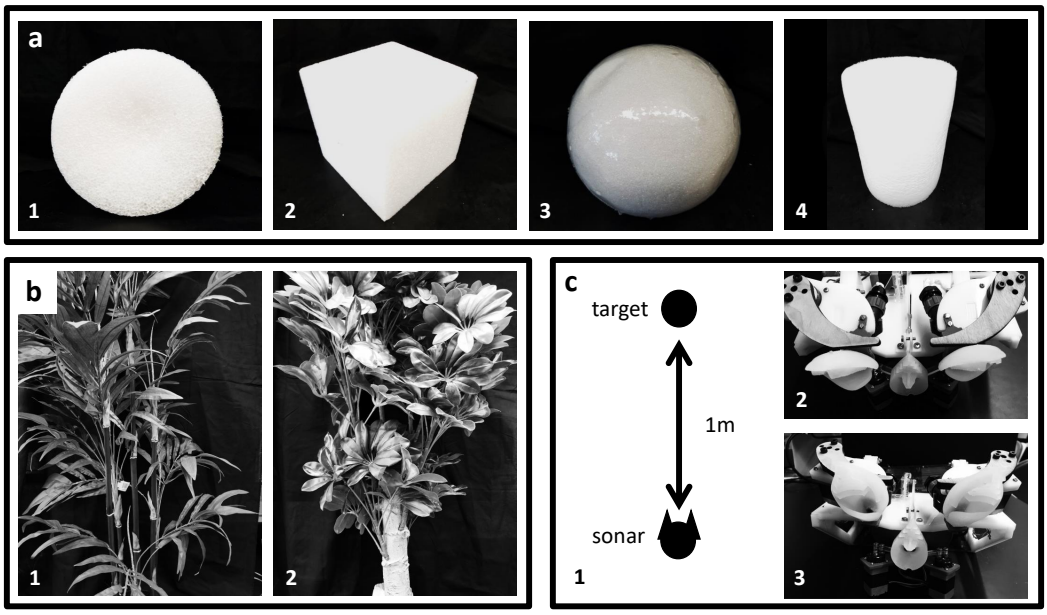

Figure 2.1: **Experimental setup and targets used in the experiments.** Targets with simple geometries: disc (a), cube (b), sphere (c), cylinder (d). All these targets had a characteristic dimension (width, height, or diameter) of 20 cm; artificial foliage (e-f). Targets were placed 1 m downrange of sonar head (g). Sonar head with lever actuation (h) and biomimetic baffles (i).

from a PVC wire strung across the top of the frame. Targets were scanned over an angular range of 80° in the horizontal at 1° resolution (Figure 2.1). A total of 250 repeat echo measurements were conducted for each sonar head orientation over an acquisition period of 10 ms. The signal used for these experiments was a 3 ms linear chirp over a frequency range of 5-105 kHz, with a Hann window applied over the entire duration of the emitted signal. The pinna and noseleaf were bent into six and three different conformation stages, respectively (Figure 2.2).

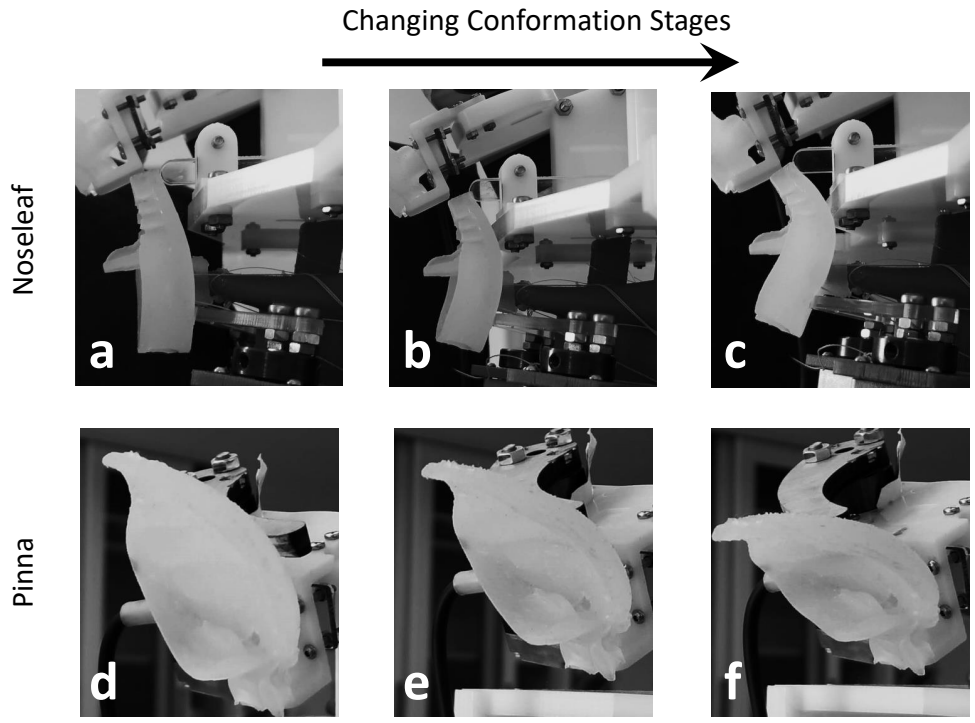

Figure 2.2: **Biomimetic baffle conformation stages.** (a-c) Changing conformations of the biomimetic noseleaf, from upright (a) to bent (c). (d-f) Changing conformation stages of biomimetic pinna in similar fashion.

2.3.3 Data Analysis

The goal of our data analysis was to analyze echo waveforms that would enter the inner ear of a bat, i.e. before neural processing takes place. Thus, methods used for echo processing designed to mimic perception, such as the spectrogram correlation and transformation (SCAT) model[84], were not used; any preprocessing was designed to reduce the dimensions of the dataset and remove noise while keeping the signal intact.

A bandpass filter (20 to 80 kHz, FIR filter design, 513 taps) was applied to all analyzed echo signals. The envelopes of the filtered signals were obtained as the magnitude of the analytic signal derived from a Hilbert transform of the input. Taking advantage of the lower

bandwidth of the envelopes, the sampling rate was reduced to 50 kHz in order to reduce the data size for the analysis.

The Hann window that was applied to the emitted chirp signal also had an effect on the shape of the extracted envelopes since the envelope of a chirp carrier multiplied by a Hann window is also a Hann window [37]. In addition, the bandpass filter applied to the waveform results in the signals being shorter in duration than the emission by about 0.5 to 1 ms due to the time-dependent carrier frequency of the chirp signal frequency.

After extraction of the echo envelopes, the data from each of the rotational scans was represented by a 5,001×81 matrix containing 5,001 amplitude samples that covered an acquisition time of 10 ms sampled at 500 kHz and 81 angular positions that covered a range of 81°, or ±40° from the center. To focus on the target region proper and prevent the recording of the initial pulse or background noise spatially distant from the target from influencing the analysis, the region in the time-angle space that occupied by the target echoes was selected manually based on prior knowledge of the target position and the echo amplitudes. The boundaries of this selection were in the same location for all targets within the same group (i.e., simple geometry or foliage targets). For the simple target geometry, cropping the resampled, filtered data resulted in a 101×61 matrix (2ms x 61°). For the foliage targets, the time dimension of the matrix was larger (151 samples, 2.5ms) to accommodate the greater size of these targets. For greater ease of the mathematical operations, each of these matrices was then converted into a vector, and all the vectors obtained for each target class were combined into a single matrix – one for simple target geometries and one for foliages each – containing every measurement (250) over the different deformation positions (18 possible conditions) for every target (simple geometries: 4 targets, foliages: 2 targets). This resulted in final matrices of 18,000×6,161 and 9,000×9,211 for simple geometries and foliages respectively. Principal components analysis (PCA, [45]) was then performed over all the samples in

order to find components representative of the variability between the targets across different targets, noseleaf, and pinna shape conformations.

Each scan was reshaped from a matrix (with dimensions of time and azimuth angle) to a vector. PCA was then conducted over all of these vectors within the data set to find which elements were responsible for the most variability across targets, noseleaf and pinna shape conformations. The analysis for the simple geometric targets and the natural targets were run separately because of the great difference in target size between these two groups. After PCA analysis, the eigenvectors obtained were sorted based on the percentage of variance they accounted for. For each of these components, an ANOVA test was run to determine whether the differences between different conformation stages were significant and whether there was an interaction between the targets and these deformation steps. Both changes to pinna and noseleaf deformation were taken into consideration, as well as combinations thereof. Since the artificial foliage was of a different size than the simple geometries, PCA and ANOVA were run separately for these two groups. The eigenvectors associated with these components were then reshaped to create a two-dimensional image, the resulting "eigenscans" (Figure 2.6) show visually where these differences manifested themselves in terms of time and direction within the target echo.

2.4 Results

The recorded echoes following bandpass filtering typically lasted 2 to 2.5 ms, and were found to be asymmetrical along the rotation axis, even for the targets with simple geometries, matching the expectation due to asymmetry within the sonar head geometry. The brightness scans of each target were visibly different from other targets. In particular, the foliage echoes differed greatly in form from the geometric targets. The peak amplitudes in the echoes from

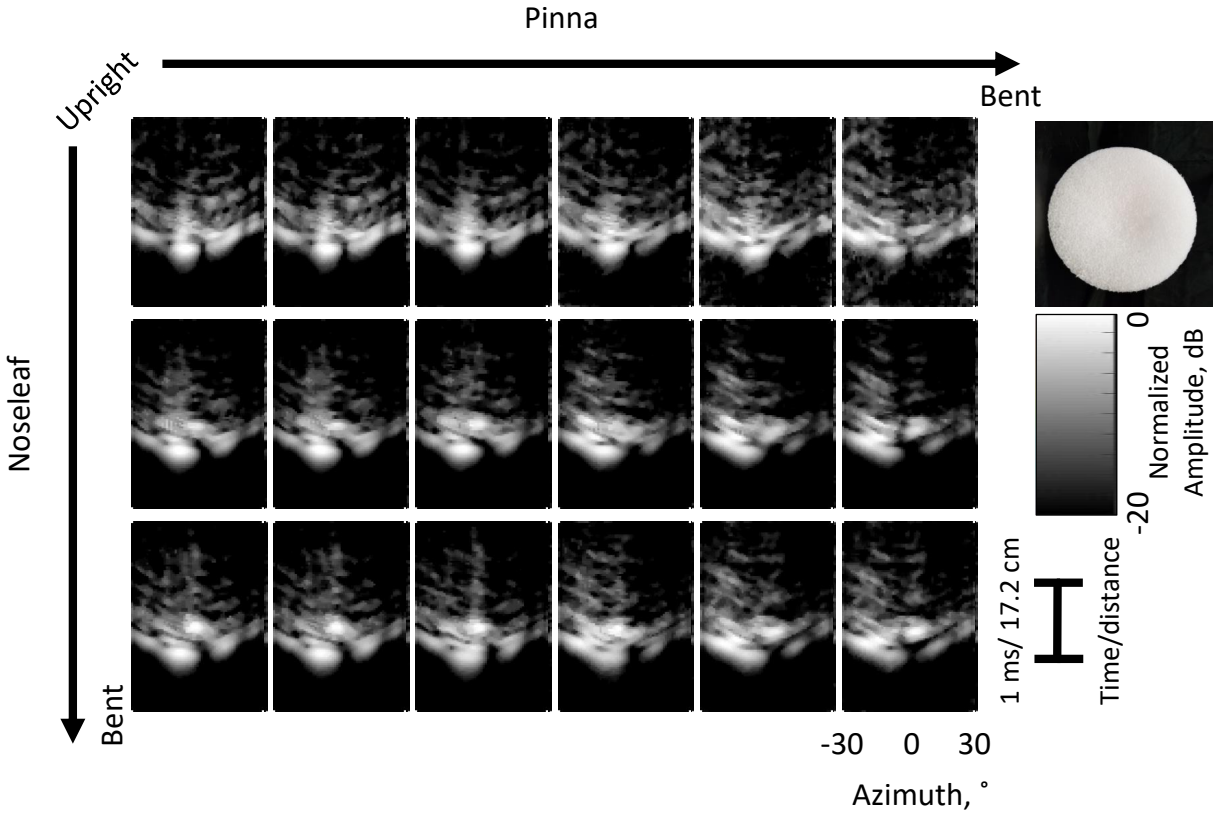

Figure 2.3: **Differences observed in echoes from a simple geometry (disc) for different baffle conformation states.** Sonar scans (brightness scans) of a simple target geometry (disc) performed with different noseleaf and pinna conformations. Noseleaf and pinna were both subjected to an increasing amount of bending (top to bottom panels for noseleaf, left to right for pinna).

the simple geometric targets occurred close to the start time of the echoes, whereas the amplitude maxima of the foliage echoes were found near the center of the echoes (likely due to the trunk of the signal).

Following PCA, the thirty components which accounted for the largest amount of variance were used for the ANOVA test, after determining that this was the number of eigenvectors responsible for 95% of the variance in the dataset. It was observed that the echo characteristics depended on the different noseleaf and pinna conformation stages (Figures 2.4-2.5).

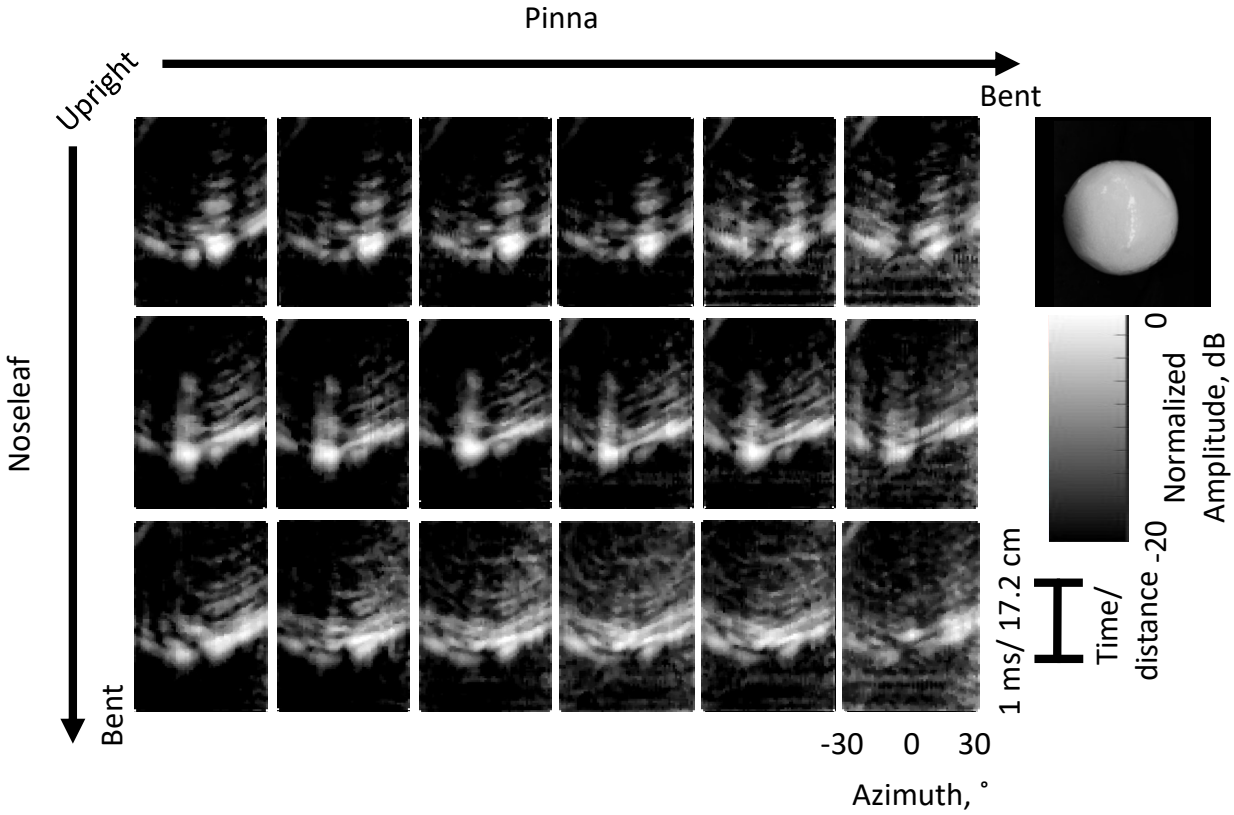

Figure 2.4: **Differences observed in echoes from a different simple geometry (sphere) states.** Sonar scans (brightness scans) of a simple target geometry (sphere) performed with different noseleaf and pinna conformations. Noseleaf and pinna were both subjected to an increasing amount of bending (top to bottom panels for noseleaf, left to right for pinna).

While these tendencies were observed in all targets; the exact nature of the changes in the echoes due to changes in noseleaf or pinna conformation depended on the targets as well.

For both geometric and natural targets there were three principal components that were found to account for significant ($p \leq 0.05$) differences between conformation stages for both pinna and noseleaf in the ANOVA (Table 2.1). Only two components led to significant differences between noseleaf positions when pinging simple geometric targets. In the geometric targets, these components were 1, 5, and 8 (for noseleaf differences, component 5

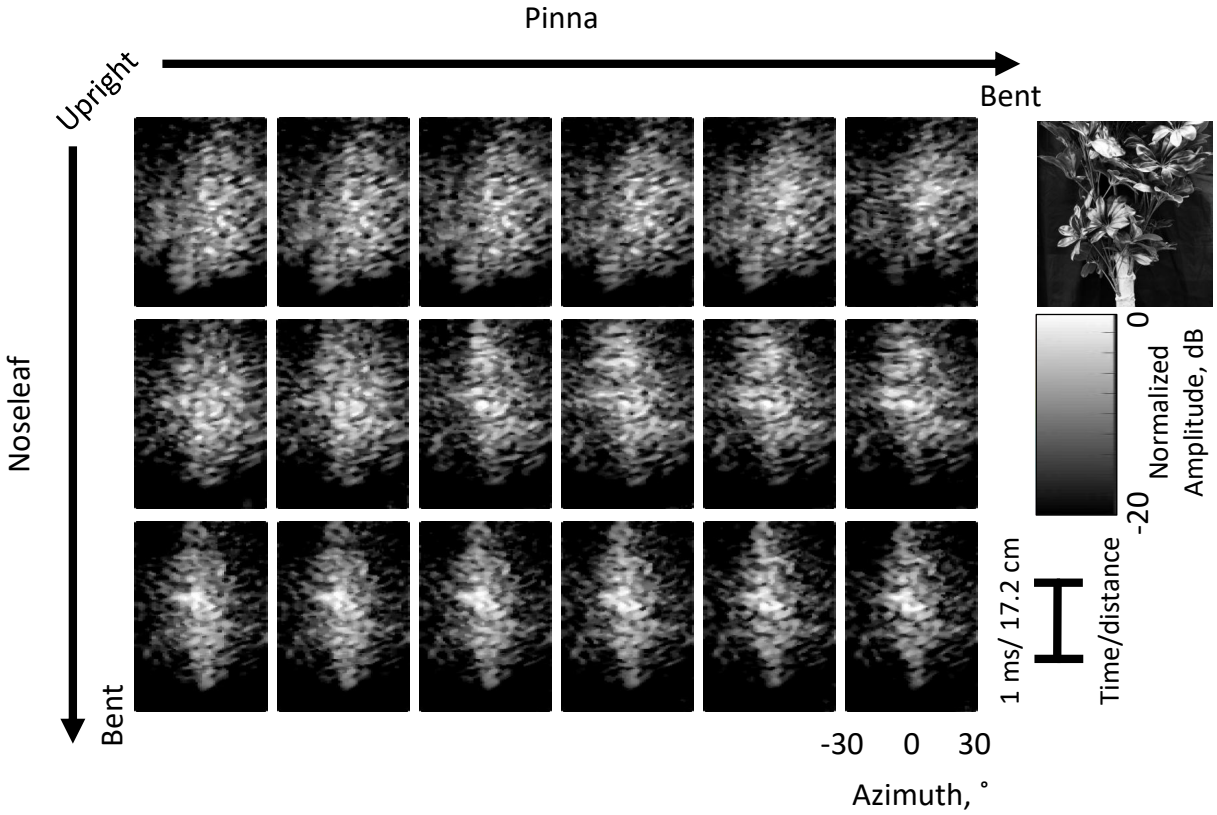

Figure 2.5: **Differences observed in echoes from artificial foliages for different baffle conformation states.** Sonar scans (brightness scans) of artificial foliages performed with different noseleaf and pinna conformations. Noseleaf and pinna were both subjected to an increasing amount of bending (top to bottom panels for noseleaf, left to right for pinna).

approached significance, but did not meet the standard where $p \leq 0.05$). These were not the same components as the ones which were observed to be significant in natural targets; these were components 1, 3, and 11. No significant results were observed in the interaction term between the different noseleaf and pinna conformation stages.

a

Principal Component Number	Condition	P-value (HF correction)
1	Pinna	~0
	Noseleaf	~0
5	Pinna	.043
	Noseleaf	.097
8	Pinna	.004
	Noseleaf	.006

b

Principal Component Number	Condition	P-value (HF correction)
1	Pinna	~0
	Noseleaf	~0
3	Pinna	..024
	Noseleaf	.045
11	Pinna	.014
	Noseleaf	.029

Table 2.1: **ANOVA results indicate significant differences between echoes of different conformation stages.** Dynamic signature detected between conformation stages in principal components of echoes from targets with both simple geometric(a) and complex (b) geometries.

2.5 Discussion

Deformations of the shape of a bat noseleaf or a pinna result in time-variant beampatterns where the emitter or receiver gain changes as a function of direction, frequency, and time. From the perspective of a scatterer placed in the field of view of such a dynamic biosonar, the changes in the beampattern function will manifest themselves in a time-variant transfer function that describes the linear channel from the emitter to the target and back to the receiver. Potential non-linear effects of motion, e.g., Doppler shifts [120], are not covered in this linear dynamic system description and can hence not be captured by the set of discrete static shape conformations that were employed here to test whether the peripheral dynamics has an effect on the echoes. Hence, the current study could lead to false negative results (i.e., no effects of the peripheral dynamics found), if the dynamic effects are limited to the non-linear domain.

For a point scatterer that is located in a single direction, the change in the beampattern

function will hence result in an equivalent change the transfer function associated with the scatterer. More complex targets can be thought of as being composed of multiple point scatterers [25, 51]. Since the transfer function describing the channel between a sonar system and a scatterer typically depends on the position and orientation of the scatter, it can be expected that the transfer functions of the individual scatterers each have independent features that could obscure the effect of changes in the emission/reception characteristics in the superposition of echo contribution from the individual scatters. Under these assumptions, it could be expected that the effect of the peripheral dynamics would be harder to detect in targets that are composed of large numbers of randomly arranged scatterers than targets with small numbers of scatterers [31].

The results presented here show that this is not the case and that strong effects of noseleaf or pinna shape conformation can be seen in the echoes – even for targets that approximate the complexity of natural foliages. Instead, time-variant components could be seen as significant echo components as indicated by the "eigenscans" (Figure 2.6). A possible explanation why the effects of the peripheral dynamics remain visible could lie in the nature of the time-variant emission and reception beampatterns. While these patterns can feature complex geometries with multiple amplitude peaks and notches [33, 117], they are – for the most part – smooth functions. Hence, time-variant effects could still have common features across echo contribution common from across the scatterers of an extended target.

It remains the subject of future research to determine whether the time-variant signatures in the echoes can convey useful sensory information, e.g., with respect to target class. Research into the random nature of foliage echoes [59, 65] has demonstrated strongly time-variant properties of these signals, that result, e.g., from successive loss of sound energy that occurs as a sonar pulse travels deeper into foliage. Hence, it may be hypothesized that the time-variant properties of the biosonar system could act as a “matching templates” for these

effects.

However, the nature of how this information would be encoded for a task such as target classification has yet to be demonstrated. The ANOVA analysis conducted here did not detect an interaction between target class and noseleaf or pinna conformation that could have served as evidence for the encoding of target class information. It should be noted that the target classes studied here were very different and hence all echoes did contain sufficient amounts of target class information for readily distinguishing between them. The contribution of the peripheral dynamics in this model may only be observable in cases where there is a significant difference between the shape of the geometries.

A linear model did not show interaction between target class and deformation stages; perhaps a non-linear model could improve results and identify interaction between target and dynamics. Additionally, adding more degrees of freedom to the robotic model, in particular the ears, could result in a more accurate robotic model to study the effects of pinnae motion. In horseshoe bats, there are about 20 individual muscles [87] which are likely to allow for significantly more complex motion patterns and conformation states than was possible with our current model of sonar head [33, 119]. Further investigation is needed to see if this complex dynamics could improve the ability for a sensing system to detect a geometric object within a cluttered environment, namely foliage. If this is the case, signatures like the one that were observed here could have the potential to increase the classification ability in small-scale sonar systems with few sensing elements by encoding additional information about a target based on its echo response at different peripheral conformation stages.

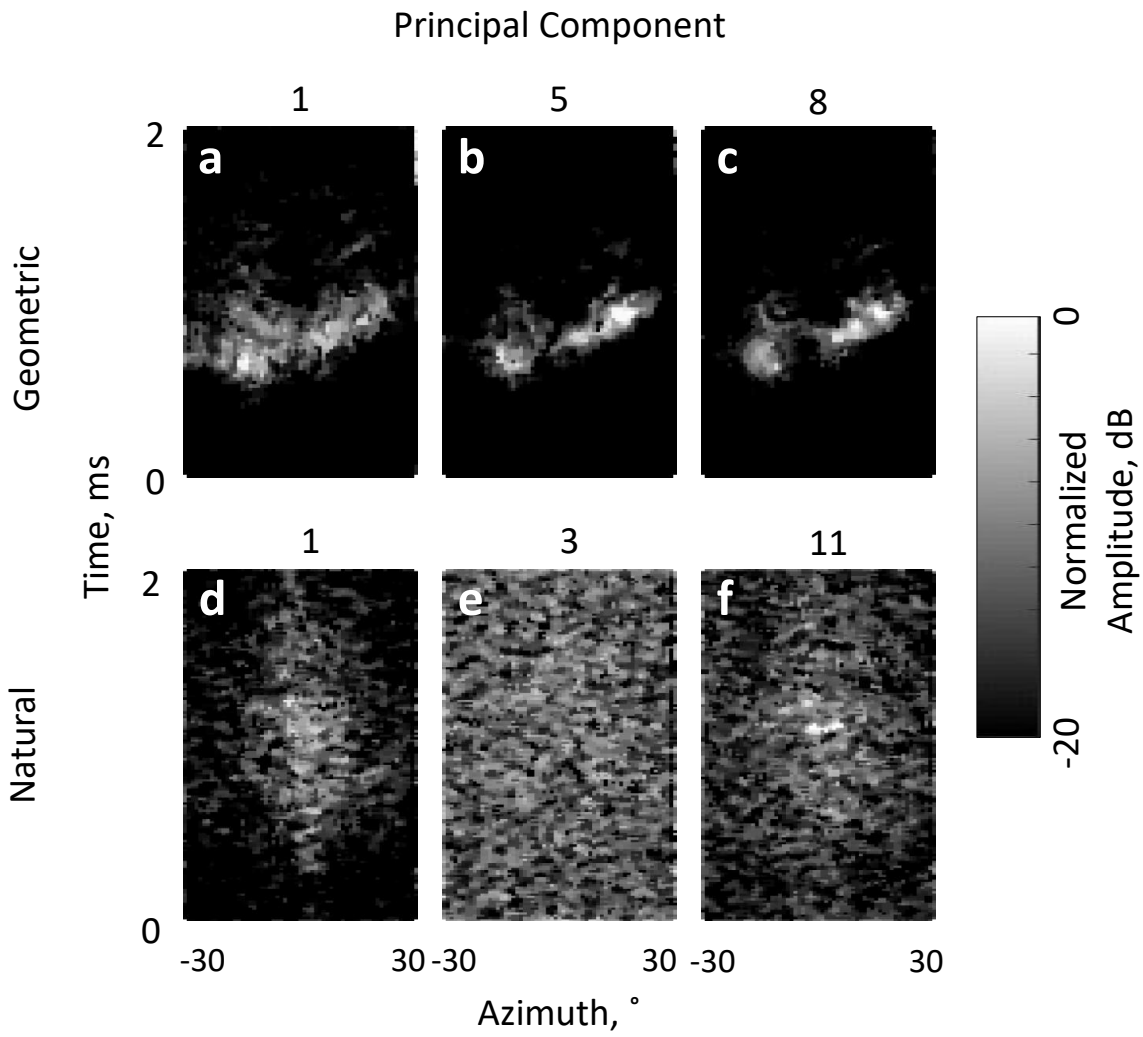

Figure 2.6: **Principal components indicate presence of a dynamic signature in echoes.** Scans regenerated from the principal components from geometric targets (a-c) and natural foliage (d-f) are used to determine if a dynamic signature is present in the echo.

Chapter 3

A biomimetic soft robotic pinna for emulating dynamic reception behavior of horseshoe bats

3.1 Executive Summary

Encoding of sensory information is fundamental to closing the performance gap between man-made and biological sensing. It has been hypothesized that the coupling of sensing and actuation, a phenomenon observed in bats among other species, is critical to accomplishing this. Using horseshoe bats as a model, we have developed a biomimetic pinna model with a soft actuation system along with a prototype strain sensor for enabling motor feedback. The actuation system used three individually controlled pneumatic actuators per pinna which actuated different portions of the baffle. This prototype produced eight different possible motions that were shown to have significant effects on incoming sound and could hence function as a substrate for adaptive sensing. The range of possible motions could be expanded by adjusting the fill and release parameters of the actuation system. Additionally, the strain sensor was able to represent the deformation of the pinna as measurements from this sensor

were highly correlated with deformation estimates based on stereo vision. However, the relationship between displacements of points on the pinna and the sensor output was nonlinear. The improvements embodied in the system discussed here could lead to enhancements in the ability of autonomous systems to encode relevant information about the real world.

3.2 Introduction

Several grand challenges in robotics are related to closing the performance gap between animals and robots in terms of achieving autonomous mobility across many environments and conditions [116]. Fundamental to achieving this is the encoding and extraction of sensory information, since any autonomous action in a complex environment can only be as good as the sensory information it is based on. Hence, the first and most basic step that needs to be taken to ensure that a robot is capable of autonomous action in a complex environment is encoding of the information that is essential to the respective task. The next step, information extraction, depends critically on the encoding step and in that it can only utilize information that has been encoded upstream [47].

A long-standing hypothesis for how the performance gap between animals and robots may be closed is that coupling sensing and actuation in a perception-action loop is critical [24]. Perception-action loops allow a robot to control the sensory information it receives in an adaptive fashion [16] Examples of how this can be implemented include the subsumption architecture, in which sensory input is fed into different levels of behavior (low to high) in the form of different processing layers [16]. Another example are robot behaviors which influence sensing, i.e., attention-driven perception-action loops spanning the system design of an entire robot [103]. Both of these models follow a bottom-up approach to artificial intelligence in which real-time processing is favored instead of a top-down approach, i.e.,

symbol manipulation [9].

Biology offers many models for powerful integration of perception and action. Particularly good examples are active sensory systems where the sensory inputs are triggered by the animals' own outputs as is the case in bat biosonar. Animals with active sensory systems have control over the emission as well as over the reception and can hence adapt both processes to maximize the utility of the received sensory information. Manipulation of sensory information encoding through physical actuation at the emission and reception interfaces is exemplified by bat species that are able to navigate in dense vegetation. Two families of bats, horseshoe bats (Rhinolophidae, 70 species [23]) and old-world round-leaf bats (Hipposideridae, 74 species [94]) in particular, stand out for unique adaptations that form a physical substrate for a perception-action loop: the animals have fast moving emitter and receiver baffle-like structures, i.e., so-called "noseleaves" [28] and the outer ears (pinnae) [33] that are deformed by highly differentiated musculatures [34, 87]. The noseleaves and pinnae of these bat species are hence examples of biological sensors that can be dynamically altered to change their responses to the input stimuli and thereby act as substrates for perception-action loops that span sensing and actuation.

Previous work has demonstrated that the noseleaf and pinna dynamics seen in bats have an acoustic impact on the the emitted and received signals respectively [33, 124]. Furthermore, it has been shown with information-theoretic paradigms that noseleaf and pinna motions encode additional sensory information that enhances direction-finding [63]. Similarly, nonlinear transformations of the incoming echoes created by fast pinna motions have been shown to result in direction-specific Doppler signatures [120]. Since some of the direction-finding paradigms used in prior work have been based on pattern recognition, it could be hypothesized that the peripheral dynamics could also support target classification/recognition tasks.

Here we introduce a biomimetic robotic sensor system for active information encoding, in

which we have realized a complete perception-action loop inspired by bats. This design is the latest in a sequence of prototypes we have designed and built to understand the impact of moving noseleaves and/or pinnae [17, 32, 67, 73, 117]. Previous prototypes have demonstrated how changing conformation states [100] and fast moving pinnae [120] can create observable changes in the acoustic characteristics of the sensory system. Some of the recent prototypes have already been tested to assess their impact on sensory information encoding in natural outdoor settings [48, 123]. However, the motions of these systems had been actuated by simple levers [100], which have limited the range of different deformations that the device can produce.

The design of the updated sensor described here has addressed the limited range of motion in the previous device while maintaining the ability for the device to be operated in mobile and especially outdoor settings. It consisted of a multi-material flexible pinna that is actuated via independently controlled soft-robotic actuators, known as pneumatic network (pneu-net) elastomers [60], to create complex non-rigid motion patterns. Pneu-net elastomers have gained popularity recently with several applications such as grasping [74, 77] since their design is inherently flexible while also remaining durable. In the current design, the elastomers were miniaturized to fit the size of the pinnae which required adaptations throughout the entire fabrication process. The elastomer-actuated pinnae were fitted with an embedded strain sensor as a substrate for feedback. Integration of all these components was achieved in a way that kept the entire robotic system portable while at the same time replicating the shape deformations seen in bats and being able to record high-quality echo signals.

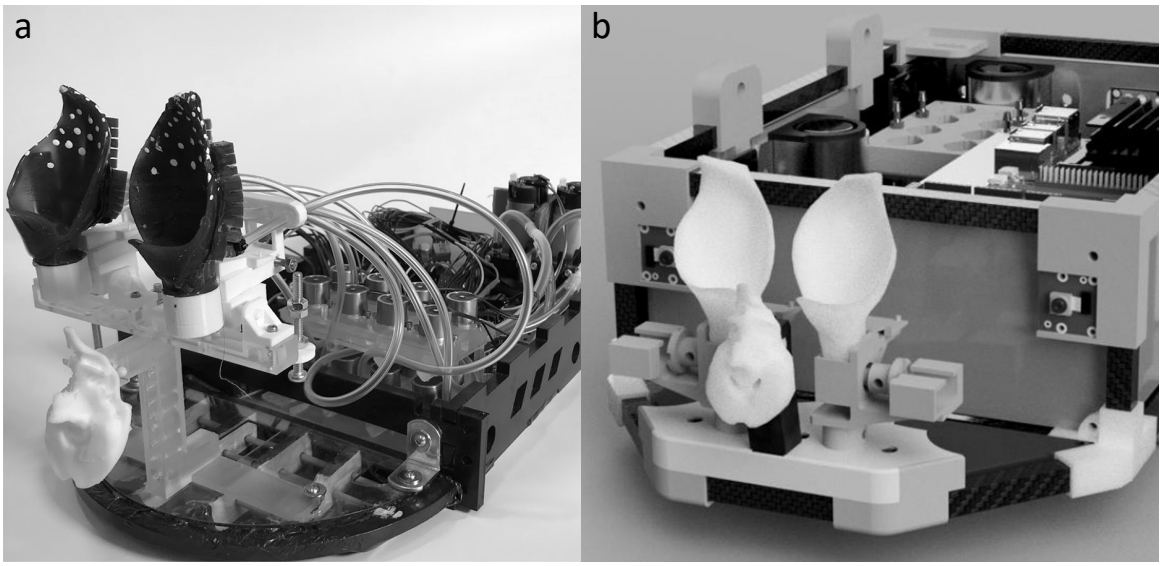

Figure 3.1: **System integration for the biomimetic sonar head:** a) integration of soft-robotic pinnae and pneumatic actuation system, b) design for the fully integrated system that also includes all control electronics.

3.3 Materials and Methods

The geometry of the pinna model was adapted from previous simplifications of the greater horseshoe bat (*Rhinolophus ferrumequinum*) pinna shape [17]. Compared to the previous version, the model used here included more detail for the antitragus [87], a flap that forms the lower rim of the pinna aperture, as well as slight changes to the overall width and concavity of the pinna to better match the geometry found in horseshoe bats. To interface the pinna model with the actuators (s. below), flat sections were cut into the back of the shape designs to provide a well-defined, uniform mounting surface for seating each actuator.

The pinna prototypes were realized using a multi-material approach to allow for large deformations of the apical portions of the shape while keeping its base and especially the microphone embedded into it stable: The majority of the structure consisted of a flexible silicone material (Eco-Flex 00-50, Smooth-On, Macungie, Pennsylvania, United States), whereas a

more rigid silicone (Dragonskin 30, Smooth-On) was used for the base of the structure. To improve visual contrast for high-speed camera recordings, the pinnae were colored with a dark (e.g., purple, black, or brown) pigment (Silc-Pig, Smooth-On); the concentration of the pigment was kept below 3% of the silicone mass in order to avoid altering the material and curing properties [5]. The pinnae were marked with a set of white points (approximate 4 mm in diameter, figure 3.1) that were distributed across its surface to facilitate motion tracking.

To realize non-rigid motions, i.e., deformations, of the pinnae, a pneumatic actuation system was designed based on the concepts of "pneu-nets", i.e., bellow-like pneumatic networks that produce bending motions in elastomers made from materials such as silicone or PDMS [60, 76]. To produce a bending motion, the two sides of the elastomer are set up to differ in stiffness [60]. The stiffness difference and hence the bending behavior of the elastomers can be influenced by virtue of parameters such as cell structure, volume, and material properties [42, 60, 90]. For the present application, some slight changes to the basic design were made, namely the addition of an airline and the miniaturization of the entire part. To ensure these changes did not affect the overall function, the elastomer deformation was simulated using a finite-element approach (Abaqus FEA, Dassault Systémes, Vélizy-Villacoublay, France) using an arbitrary load since the exact amount of pressure in the system was not known prior to manufacture (figure 3.2b). To provide a boundary condition for these simulation, a fixed corner beneath the intake tube of actuator furthest from the balloon cells.

The design of the elastomers could be simplified taking advantage of the integration with the pinna structure. Prior work had employed an inextensible layer that was stiffer than the extensible layer [60]. Here, the bending motion was accomplished by virtue of the one-sided loading of the elastomer by the pinna in conjunction with the elastomer's geometrical parameters. Hence, top and bottom layer of the elastomers could made from the same material (EcoFlex 00-50, Smooth-On [3, 4]).

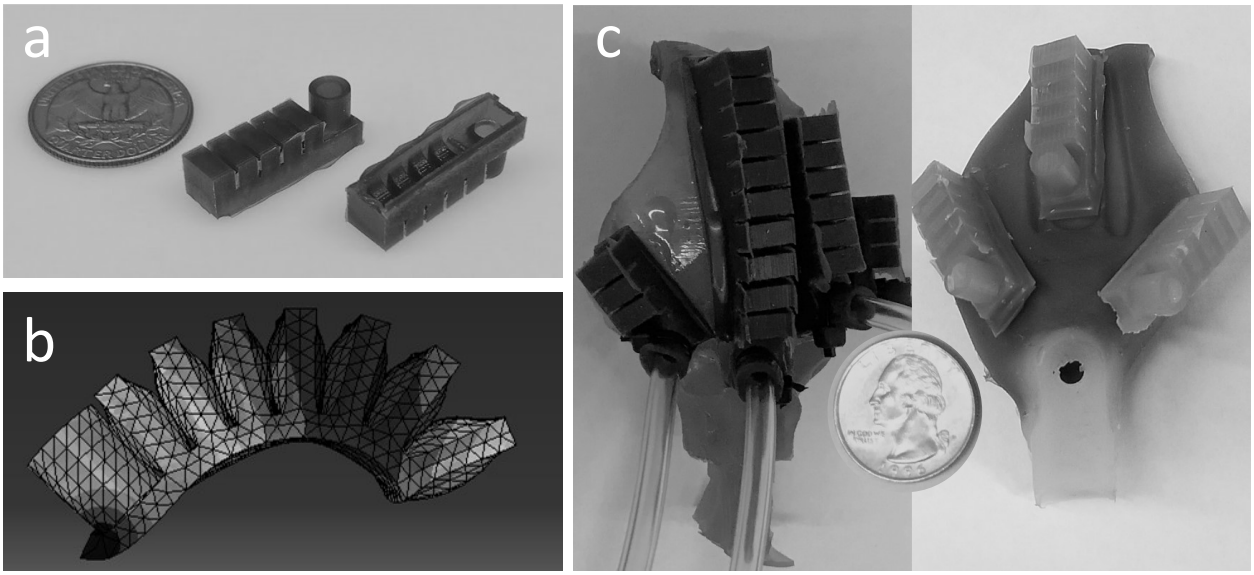

Figure 3.2: **Elastomer design for the sonar head's pneumatic actuation system:** a) Top layer of a five-cell elastomer; b) elastomer finite-element model for simulation of bending; c) elastomers of different lengths placed on two silicone pinnae. The design of the pinna on the right was used in the final design.

In the work presented here, each pinna was fitted with a set of three elastomers (figure 3.2c). Each of these elastomers consisted of five cells (figure 3.2c), was 27 × 10 × 7 mm in size, and had its own, separate connection to the air delivery system. The air delivery system was designed to drive all elastomers while keeping size and mass as low as possible. The air was supplied by two miniature air compressors with an integrated compressed-air reservoir (1410 vd series, Gardner Denver Thomas, Sheboygan, Wisconsin, United States). A system of low-profile proportional valves (VSO LowPro series, Parker Hannifin, Cleveland, Ohio, United States) was used to control the air flow to the elastomers. Each elastomer was controlled by two valves, one to regulate the inflow into the actuator and the other to regulate the outflow. A manifold system was designed to route the tubing between the compressors and the elastomers. The manifold design was realized in resin using an SLA printer (Form 2, Formlabs, Somerville, Massachusetts, United States). Each valve unit had a "two-ports, two-positions" conformation to allow for fill and exhaust valves to be controlled independently.

Each fill valve received its input from the compressor directly, its output was split between the actuator and exhaust valve (figure 3.3a). The tubes connecting the control valves to the elastomers were held by a bracket on the back of the pinna to reduce the range of motion of the tubing during filling and exhausting. A manifold (figure 3.3b,c) was used to contain the valves and simplify the overall system. The design features pneumatic routing within the part and is printed using stereolithography (SLA) 3d printing (Form 2, Formlabs, Somerville, MA). During post-processing of the manifold, the air ducts inside the part were flushed with isopropyl alcohol to prevent any uncured resin from solidifying and clogging the ducts.

The airflow through the proportional valves was controlled by virtue of a pulse-width modulation (PWM) input that was applied to the valves' duty cycle. To accomplish this, the duty cycles were mapped onto an 8-bit representation clocked with a PWM frequency of 31 kHz. Due to the additional stiffness provided by the pinna baffle, the dynamic range for pinna deformations fell within the upper 30% of the PWM controller's total dynamic range. A MOSFET amplifier was used to drive the control input of the valves (12V peak-to-peak). To test the impact of actuating different combinations of elastomers placed on the pinna, the respective valves were operated to fill each elastomer for 25 ms and then exhaust it for 75 ms. During these experiments, each actuator was either turned on using this filling and exhausting pattern or left turned off entirely.

In order to quantify the pinna motions produced by the actuation system, a stereo pair of high-speed video cameras (Chronos 1.4, Kron Technologies, Burnaby, British Columbia, Canada, operated at a frame rate of 1069 Hz) was used to create three-dimensional reconstructions of the deforming pinnae. Three different motion conformations (figure 3.4) were recorded in this way. The motions of the landmark points were tracked using a Kalman filter estimator (DLTdv digitizing tool, [40]). Where automatic tracking failed, the point locations were identified manually. The distance traveled for a given point was then calculated as the

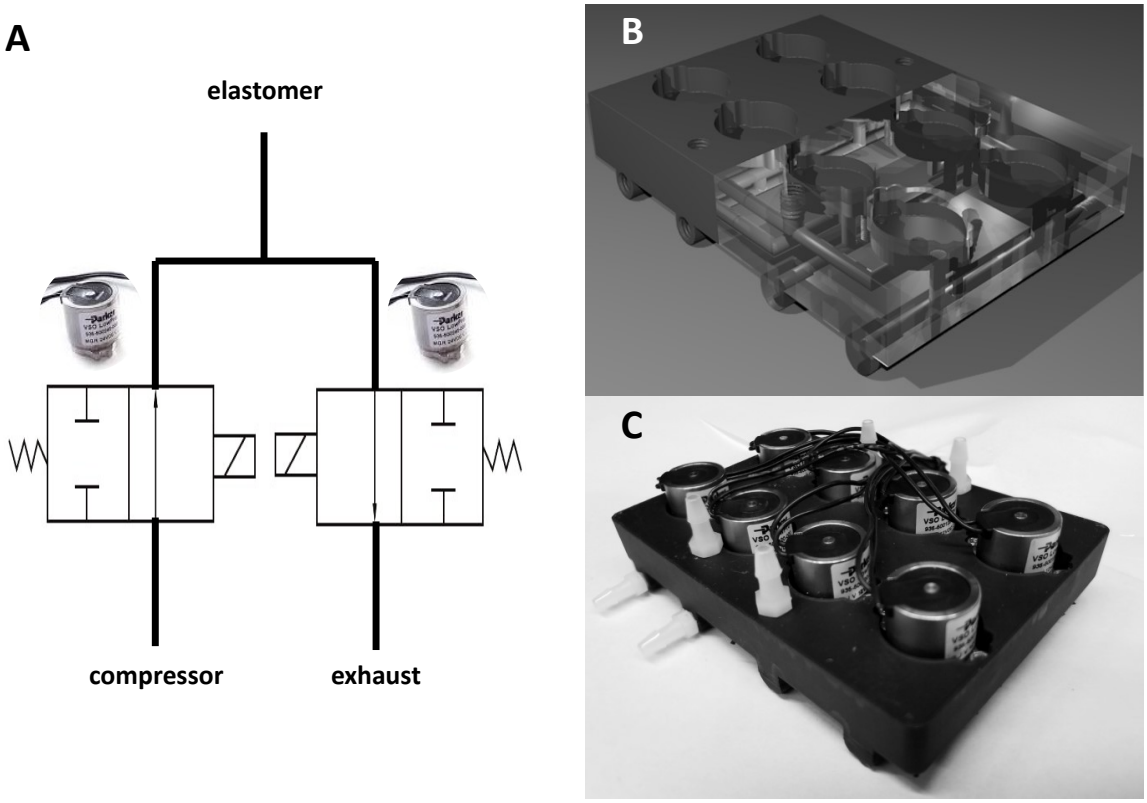

Figure 3.3: **Pneumatic actuation system for soft-robotic sonar head:** a) A microcontroller controls each actuator via a pair of valves joined in series. By default, each valve is closed; To fill the actuator, the fill valve is opened and releases air sourced from the compressor, when exhausting, the fill valve is closed and the exhaust valve is opened, sourcing air from the actuator; b) Rendering of the manifold model illustrating the inner tubing used to control airflow to the different elastomers; c) printed manifold with attached valves. A total of 8 valves can fit on this manifold design, which allows for independent control of four actuators.

magnitude of the distance traveled from the point on a specific frame to the next. These values were then compared to the results from the nylon strain sensors.

To enable future work on closed-loop control of the deforming pinnae, soft sensors [126] were tested as a way to measure strain in the deforming pinnae. These sensors are a relatively new device and are smaller, lighter, and less expensive than many other types of flexible sensors [27]. The sensors measure strain by virtue of a change in the resistance of a coiled

wire that results from compression or elongation of the coil [7, 126]. The material used was a 2-ply silver-coated nylon with a linear resistance of less than 3,000 $\Omega/_{m}$ (117/17 dtex 2ply +B, V Technical Textiles, Palmyra, NY, [91]). To manufacture the sensors, a 50 cm piece of the thread was loaded with 0.5 N and rotated 555 times in order to create a coil with 11.1 windings per cm of length. A current (0.3 A maximum) was then passed through the sensor (V_{cc} = ∼22 V) in 350 pulses of 100 ms duration each in order to anneal the sensor, thus making its coiled state permanent.

To test the sensor response on a deforming pinna, a simplified version of the pneumatic pinna was used (figure 3.6a) that was made of single silicone material and equipped with only a single elastomer in the center. This was due to the fact the sensors have been previously tested in only simple silicone structures [7]. The sensors were attached to the back of the pinna in two different ways: The first was to place the sensor around the rim of the elastomer's footprint, then sealing the elastomer in place with silicone. In the second approach, the sensor was cured in silicone in a special mold which was then placed under the elastomer when curing the inextensible layer on the back side of the pinna. In either case, the pinna was clamped at the base during testing. The sensor output was read as a voltage (between 0 and 3.3 V) using a voltage divider circuit with the sensor acting as one of the resistors in that circuit. The sensor output was digitized at a sampling rate of 1,000 Hz and with 12-bit resolution (Arduino Due, Arduino, Ivrea, Italy). During each experiment with the sensors, the pinna was recorded with a stereo pair of high-speed video cameras as described above. Recordings from the sensor and the video cameras were triggered at the same time and were aligned for analysis.

To test if the observable effects of changing pinna state can be seen in acoustic signals received by the system, recordings ($N = 50$ per motion profile) were taken of a 15 ms, 35 kHz constant-frequency pulse from a MEMS capacitive microphone (Momimic, Dodotronic, Italy) placed

inside the "ear canal" of the pinna baffle. Data was recorded using a 12-bit data acquisition system (PCIe-6358, NI, Austin, Texas, United States). To compare the time courses of the signal amplitudes, all the data was normalized with reference to the maximum amplitude recorded across all trials.

3.4 Results

All actuators manufactured in this research successfully performed the typical curling motion of pneu-net elastomers. When tested without a pinna attached, the elastomer's balloon cells expanded to between 2.5 and 3 times their size at rest. No failures were observed in the unloaded elastomers during approximately 40 hours of continuous testing by inflation/deflation. Loading with the pinna structure changed the inflation behavior of the elastomers: It was observed that some cells, in particular the cell that was the second to most distant from the air inlet, expanded to slightly more than three times their size at rest. The locations of the larger inflations corresponded with those of the few instances of observed failures that typically occurred after a few thousand inflation cycles.

Each of the eight different combinations of open and closed valve states produced a unique motion pattern (figure 3.4). Regardless of valve state, a single deformation took approximately 75 ms to complete and was followed by an additional 225 ms to return to the resting state. The displacement magnitude at the pinna tip was observed to have a mean of 24.6 mm (standard deviation 0.5 mm, N=140). We observed differences in acoustic recordings in the reception of the signal with the change in deformation (figure 3.5). There were distinct differences in the sound level of the signal as well as its time shape, observed by analyzing the fundamental and first harmonic of the signal. This was especially obvious when compared with the no-motion case. Using all three actuators simultaneously has the most obvious

effects on signal amplitude, especially in the case of the first harmonic, which was 25 dB louder than its no-motion counterpart. The envelope shapes obtained for the fundamental as well as the harmonic both depended on the pinna deformation pattern. In addition, the relationship between the enveloped of the two frequency components where also affected by the different deformation patterns. All these differences were observed in the region of the recorded pulse itself and were much larger than any slight variations due to noise. Additionally, slight variations in the frequency content of the fundamental and first harmonic were observed.

The responses recorded from the nylon sensor were found to reflect the deformation of the pinna baffle. The sensor and camera data was shown to be highly correlated (correlation coefficient 0.97, standard deviation = 0.001, $N = 12$ repetitions). When considering the entire deformation cycle of the pinnae, the sensor responses were clearly highly nonlinear (figure 3.6b). However, the sensor response remained approximately linear for low velocity and small displacements (figure 3.6b, III-V); the region of greatest nonlinearity coincided with the highest pinna velocity and the greatest displacement (figure 3.6b, I-II). While strongly nonlinear overall, the relationship between the pinna position and sensor response remained consistent between trials. We observed the sensor response to motion in two independent pinna prototypes (140 trials total, i.e., 70 per pinna). There were fewer trials when collecting camera data since the cameras could only record in 8 s intervals, compared with 45 s intervals that the sensor could be recorded. Both recordings start at the same time, and are synced this way. There was no statistical significance between the data sets from the two pinnae (two-tailed t-test, $p = 0.21$, $N = 140$ observations equally sampled from the two pinnae).

3.5 Discussion

Creating soft-robotic pinnae based on pneu-net elastomers has required making several trade-offs: Elastomers with more cells tend to have a smoother curling motion and will expand less at each individual cell [60]. Longer elastomers can also create larger displacements and velocities. However, adding additional cells – and thus lengthening the elastomer – resulted in inconsistencies in the distribution of the airflow, with air passing more to some cells than others. In addition, long elastomers do not permit local control of the pinna shape. In terms of material properties, interfacing the elastomer with the pinna allowed the use of single material since one-sided loading by the pinna had the same effect as a greater stiffness of the inextensible layer [60, 77].

Finally, there are trade-offs related to the number of actuators placed on the ear. In theory, more independently-controlled actuators give the user more degrees of freedom, but in practice this is not always true. Designs using four actuators were rejected due to the effects of the fourth actuator being masked by the other three. The impact an additional actuator may or may not have is important to consider, as more actuators require more hardware (the current system uses a pair of valves to control airflow) and more electrical power to operate them.

The elastomer designs tested here were able to perform with relatively few failures. The potential for failures did increase when the elastomers were placed on the pinna but it was found that with a favorable positioning of the elastomers the failure rate could be reduced, with the latest version only having one failure occur thus far. Failures could also potentially occur if a manufacturing error was not caught, this would occur typically between two cells or at the air supply location on the extensible layer.

The independently controlled actuators used in the present design were able to produce

eight visibly unique bending profiles providing a level of control over the pinna deformation that is significantly greater than what has been achieved in previous versions of the sonar head [17, 100, 117]. Additionally, interactions between the simultaneous inflations of different elastomeres were observed that could be the result of changes to the load of one actuator through the action of another. These interactions could make controlling a soft-robotic pinna harder, but could also be used to create an even greater range of different deformation patterns. The range of possible motion patterns could be further extended by varying the time courses of the pressures that are applied to each elastomer and their relative timing. However, utilizing temporal differences between the pressure inputs will be limited by the lowpass characteristics of the elastomers and their pneumatic inputs.

Given the positioning of the elastomers along the back of the biomimetic pinnae, the different pinna deformation patterns obtained in the current work all resulted in opening or closing of the pinna aperture. This is qualitatively similar to the pinna deformations seen in rhinolophid [33] and hipposiderid bats [119]. However, it remains to be seen whether the differences that were created by the different activation patterns for the elastomers have an equivalent in the pinna deformations of bats. The rigid motions of bat pinna have already been shown to display a large amount of variability [79] and qualitative observations suggest that the deformation are also variable. The exact nature of the variation in the deformations and its possible functional significance have yet to be determined.

The nylon coil sensors were selected for this design due to their small size, low weight, and low cost that sets them apart from many other force sensors, such as piezoelectric sensors [27, 96, 126]. In our model, the responses of the embedded strain sensors were shown to be very consistent across multiple recordings with the same pinna as well as different pinnae. It was found that there are multiple components to determining this, in particular during rapid acceleration of the sensor. These components consist of an approximately linear

response vs strain paradigm which is the basis for the sensor function itself [7], as well as a nonlinear element most likely due to the properties of the material itself, in which the physical pulling apart of the charged metal particles in the material is initially dependent on the speed of the sensor motion [14]. Other types of sensors with similar shape and mechanism have been shown to provide an accurate response when multiple sensors are combined; this could be a potential solution to some of the problems discussed here [44]. This may increase the complexity of fabricating the pinna, as it would be significantly harder to route the sensor in an optimized way without threading it in some complex manner through the pinna structure.

Additionally, a closed-loop control algorithm still needs to be developed in order to take the sensor response and equate this to commands to control the valve state. While the nylon sensors seem to be a potentially useful and reliable way to acquire information regarding deformation, further work will need to be done to connect the readings from the nylon sensors to the on-times and duty cycles of individual valves. Each sensor was slightly different, while the signal response is very similar there are slight dc shifts between each sensor which needed to be considered when evaluating the response, however we have shown precision in manufacturing can alleviate these effects, as observed when two different pinna with different sensors performed in a significantly similar way. In addition to signal processing methods of obtaining this, improved sensor integration, perhaps by finding ways to further reduce the total amount of space covered by the sensor under the pinna will give a response to a more localized region, which we believe is the most useful way to get meaningful data from these sensors. Additionally, the sensor response can be improved if the axes of rotation were fixed in a way that the sensor could only bend in a single direction. Other forms of control algorithms that may be useful when considering some of the problems and limitations of the current system include behavior-based approaches such as using neural networks [11].

A continuing challenge regarding this technology is to integrate it into a new sonar system, where additional components have to be considered. Our system consists of some higher power lines, for speaker systems and motors. These parts are kept in very close proximity. This is why analog signal lines are kept as small as possible. Use of high-pass and low-pass filters can also be an effective means of preserving the integrity of small analog signals [80]. Litz wire, designed to pass a limited frequency bandwidth of an AC signal [92] is a viable option for integration in the overall system.

Acoustic noise and signal preservation is important to the integrity of the system. It was ensured that the pneumatic pinna system did not create high frequency noise and that the inflated elastomers did not affect the reception beampatterns of the pinnas in a significant way. The valve system was observed to in a slight way influence the microphone system and was thus moved a further distance away. The effects of the deformation on the acoustic properties of the pinna detected here are in line with previous observations of similar effects on the emission side [117]. The small changes in the carrier frequencies are possibly due to Doppler shifts which have been shown to act upon incoming signals while the pinna is in rapid motion [120]. While the differences that have been qualitatively observed here have an impact on the encoding of useful sensory information encoding is a topic for future research efforts.

3.6 Acknowledgments

This research has been supported by the Naval Engineering Education Consortium (NEEC, contract number N001741910001) and the Office of Naval Research (ONR, MURI N00014-17-1-2736).

We would additionally like to thank Matthew Conk, Emmett Eckman, Prerit Kwatra, San-

meel Lagad, Sierra Lunsford, Charlie Martin, Kent Sullivan, Brandon Walker, and Yanhao Wang.

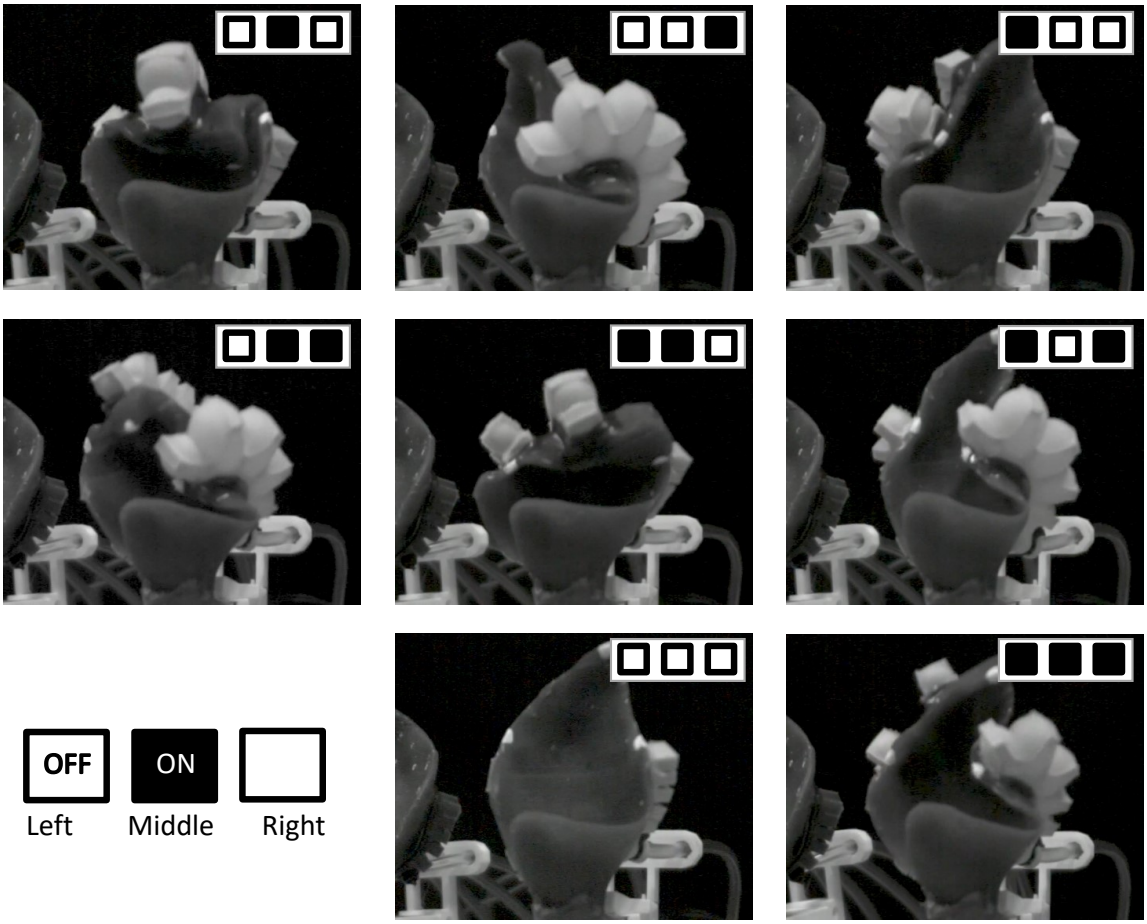

Figure 3.4: **Different pinna deformation patterns were obtained for different activation patterns for the three elastomers:** For each deformation pattern, the maximum displacement state is captured in the images. Each actuated ("on") elastomer was filled for 25 ms and then exhausted for 75 ms.

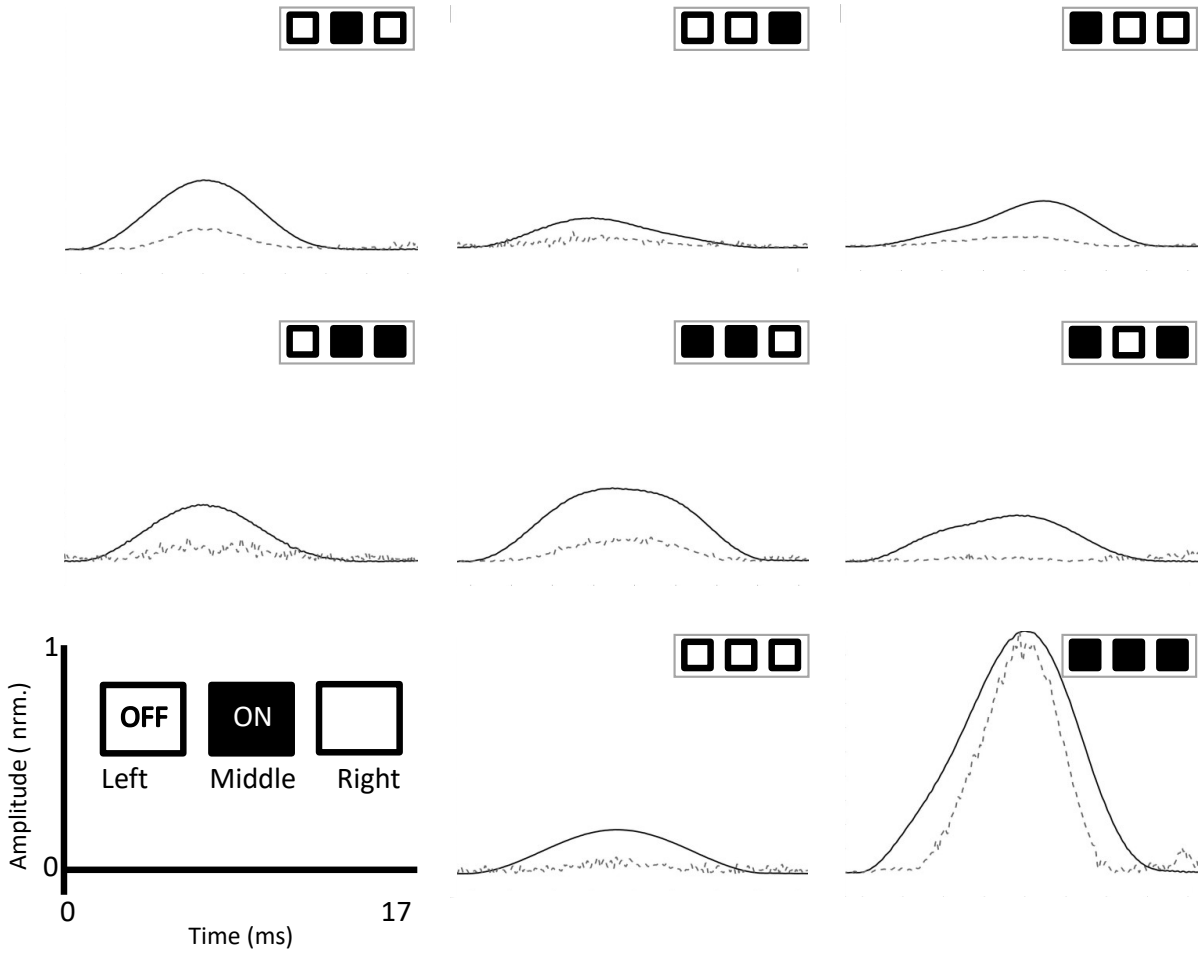

Figure 3.5: **Acoustic impact of different pinna deformation patterns:** Comparison of signal envelopes fundamental (black) and first harmonic (gray, dashed) modulated by different pinna deformation patterns (see figure 3.4). The pulse had a duration of 15 ms, and contained two frequency components, a 35 kHz fundamental and a first harmonic at 70 kHz. It was emitted 1 m downrange from the pinna. Each envelope was normalized by maximum envelope amplitude obtained across all trials and motion conditions. Each plot shows the average envelope function for the respective motion profile ($N = 50$ per motion profile).

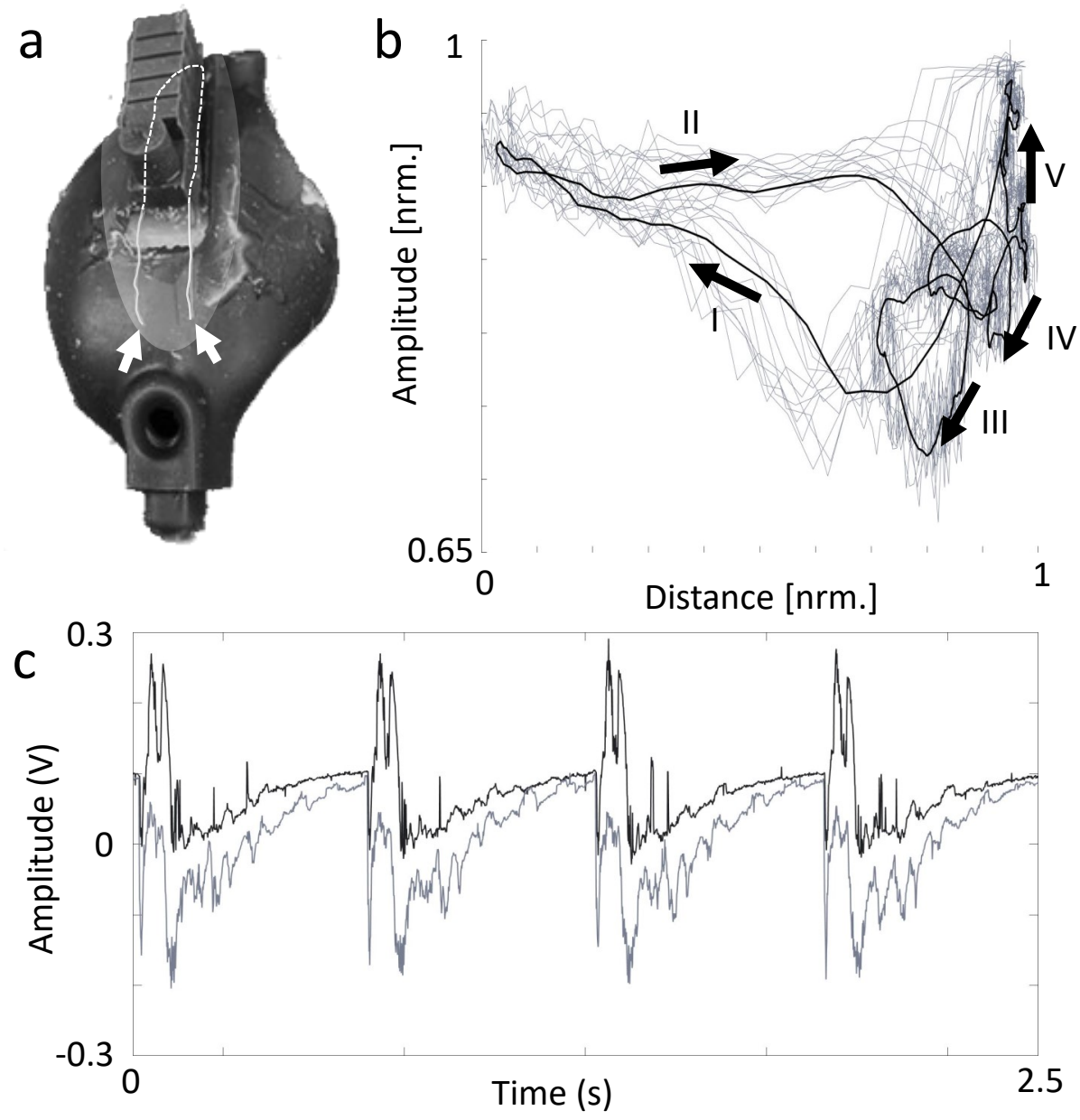

Figure 3.6: **Soft sensor integration and response:** A: Nylon sensor (see arrows) placed on a pinna for testing. B: Comparison of amplitude in sensor response (normalized voltage) to pinna position (normalized magnitude of pinna position). Response was observed to be very nonlinear across regions I and II and becomes more linear as it approaches rest (i.e., III-V). C: Comparison of two different pinna/elastomer/sensor systems shows relative similarity and extremely high correlation (correlation coefficient 0.99)

Chapter 4

Summary and Conclusions

4.1 Research Accomplishments

There are gaps in current navigation and sensing technology, especially as they apply to small-scale robotic systems. Bats provide a unique model for being able to identify a large amount of features using a few "smart" sensors as opposed to many simple sensors. Biomimetic models of bats have indicated the importance of changing conformations and motions of dynamic emitters and receivers influence incoming sound and could provide additional features to improve sensing capability using fewer sonar elements.In order to further the capabilities of these models, the hardware must first be upgraded to allow for the capability of the system to be expanded. This was done in two major ways. First, the biomimetic baffles of the system were updated to more resemble those of *R. ferrumequinum*. This can be seen in the addition of the antitragus of the pinna, as well as the overall noseleaf shape has been heavily changed in order to have similar nostril shapes and furrows to that of *R. ferrumequinum*. Additionally, the actuation was improved to allow for more degrees of freedom, using a pneumatic actuation system. Finally, a prtototype soft sensor was designed and tested on a biomimetic ear, which will lead to further developments in sensing.

The data collected from systems using these critical hardware updates sought to show the advantages of adaptations in the bat biosonar system and provide a case for these adaptations to be considered for bioinspired navigation system design. This work provides a strong case

for the use of dynamic acoustic baffles to further the capabilities of sonar navigation and unmanned system navigation by providing unique features which can be used to extract more information from the surroundings using fewer sensors. This has been shown in two ways. First, the changing conformation state of biomimetic pinna and noseleaf baffles illustrate signatures encoded in echoes of both simple and complex geometries. Second, with the introduction of a novel actuation system for the pinna baffles, it was shown that each motion could create a strikingly different response to the same sound source. This was illustrated not only in the fundamental, but additionally in the harmonics.

4.2 Discussion

This work has the goal of using biomimetic paradigms; as such it allows for both a better understanding of the model organism while also using the structural and mechanistic paradigms of this organism to further technological advances [13].Specifically, this is accomplished as the work sheds light on the physical paradigms of the dynamic biosonar systems of horseshoe bats. Previosly, the effects of doppler shifts had been shown to aid in localization of objects [120], attention-driving mechanisms, and even in social behavior of bats [113]. It had not been determined whether the effects of the dynamics had effects to the overall shape and structure to the echo outside its main lobe, whether the scattering or absorption effects of high frequency sound [104]would minimize any significant effects of the motion. These observable effects respective to both azimuth and time shed light on possible ways bats can distinguish different objects from others in their surroundings. This hypothesis is currently been supported by data collected from foliage echoes indicating dynamics has a role to play in discerning different types of forests from each other [48].

As the need for robotic system moves towards adaptive systems [55], new design paradigms

need to allow for the system to be adaptable. This is critical for the design of the dynamic pinna and noseleaf system for the sonar head. The main elements for this system consist of acoustic baffles, motor system, and motor feedback.

First, the acoustic elements were updated to try to best mimic the properties of the bat. First, more detail was put into the structure of both the pinna and noseleaf systems, highlighted by the addition of the anitragus into the pinna system [100], and the design of muli-material ears to allow for complex motions without sacrificing stability [101]. Adding degrees of freedom to the pinna and noseleaf motion allows for expansion in the capabilities of the system; to do this, different options were analyzed, including motors and pneumatic actuation. Using motors has several benefits. Regardless of what type of motor is being used (DC, servo, stepper), they tend to be easy to program, follow simple to understand motion trajectory (usually a simple rotation), and are easy to mechanically attach to the system [21, 75]. However they are limited in their total range of motion to a single axis (making the design decidedly less less-lifelike), often require more power and are heavier when significant torque requirements are present.A pneumatics approach by comparison is less limited regarding the motions that can be created and can be directly interfaced with silicone baffles easier, less power required at higher torques, smaller overall mass close to baffles. However, they are harder to program, require careful distribution of airlines, and are harder to manufacture properly [99]. We found the pneumatic system provides more opportunity to look at changing conformation state in the ear by looking at interactions between sound and motion profiles. For replicating rigid motions observed in bats [79], using motors may be the better method as the motion is more linearly defined.

The prototype sensor system could be a possible answer for addressing challenges in proprioception and motion control, which is much more difficult in soft actuation systems compared with more conventional rigid ones [112]. This would allow for further expansion of imple-

menting behavior-based systems, which have been demonstrated to be able to allow for faster responses to complex tasks [10, 11], and have been illustrated to be able to be used to further understand the information flow in a perception-action loop [50]. Implementing accurate control in a soft system could further other applications that require accuracy and precision, such as tools being developed for laporoscopic surgeries [82], robotic exoskeletons for rehabilitation [77], or crawling/mobile robots [19]. A sensor-response algorithm still needs to be developed, which is hindered currently by non-linear components due to the material properties of the conductive nylon [14]. Adding more sensors may help this, as has shown to be the case in a sensor of a similar conceptual design (though different material) [44]. Behavior-based approaches could also be a possible solution as the control algorithm could account for the time-dependent properties of the material.

4.3 Conclusions

As the current state-of-the-art sensing systems lag behind biological systems in their ability to aid in autonomous navigation [86, 102], it is only logical to look to new design paradigms to develop more capable systems, both at a hardware and software level. Bioinspiration and/or biomimcry has allowed for the study of how living organisms accomplish similar tasks to inspire new methods of accomplishing these tasks [13]. This work has taken inspiration from the adaptations of horseshoe bats to characterize the physical properties of dynamic pinna and noseleaf motion and understand how this adaptation could be used to encode additional features for improved sensory systems. To accomplish this, the capabilities of the sonar head were greatly expanded from previous systems, with the addition of biomimetic structures with more degrees of freedom and the beginnings of a fast-acting motion feedback system. These accomplishments provide insights into the potential for improvements to

sensing modalities by taking inspiration from bats using dynamic biosonar systems.

4.4 Recommendations for Future Work

The development of the sonar head over the course of the previous two versions greatly expanded the experimental capabilities of the biomimetic sonar head and has already lead to multiple publications [48, 100]. The next version of the sonar head should further press the possibilities for work to do be done here, and the following are recommended for updating the hardware of the system:

- Use the sonar head on a system in flight: It has been a goal of the lab for some time to use the system on a flying vehicular system such as a drone.
- Update data acquisition system to allow for longer acquisition period without significantly lowering the sampling frequency.
- Refine actuation and emitter systems to consume less power. This may require exploring alternative actuation mechanisms (such as using microfluidics or tendons) and continuing to explore different emission methods.
- Integrate the sensors into a feedback loop, perhaps using a behavior-based system.

Additionally, the following are recommended experiments to further exploration into the effects of dynamic peripheries on echoes and the relationship between perception and dynamic sensors:

- Use sonar head to analyze how different motion profiles affect responses from unique targets.

- Let the sonar head iteratively alter the motion profile in order to maximize a given signal characteristic, then observe the similarities and differences of these profiles across several targets or signal conditions.

Bibliography

[1] (2000). *Reson Seabat 7125 High Resolution Multibeam Echosounder*. Oceanscan.

[2] (2012). A novel biomimetic sonarhead using beamforming technology to mimic bat echolocation. *IEEE Transactions on Ultrasonics, Ferroelectrics, and Frequency Control*, 59(7):1369–1377.

[3] (2018). *Ecoflex Series: Super-Soft, Addition Cure Silicone Rubbers*. Smooth-On.

[4] (2019a). *Dragon Skin Series Addition Cure Silicone Rubber Compounds*. Smooth-On.

[5] (2019b). *Silc Pig Pigments*. Smooth-On.

[6] (2020). *4200 Side Scan Sonar System User Hardware Manual*. EdgeTech. 0004842_REV_N.

[7] Abbas, A. and Zhao, J. (2017). A physics based model for twisted and coiled actuator. *2017 IEEE International Conference on Robotics and Automation*.

[8] Anupam Gupta, D. W. and Müller, R. (2015). Interplay of lancet furrows and shape change in the horseshoe bat noseleaf. *The Journal of the Acoustical Society of America*, 138(5):3188–3194.

[9] Arkin, R. (1998). *Behavior-Based Robotics*. Cambridge, Massachusetts: The MIT Press.

[10] Armbrust, C., Proetzch, M., Schäfer, B.-H., and Berns, K. (2010). A behavior-based integration of fully autonomous, semi-autonomous, and tele-operated control modes for an off-road robot. In *2nd IFAC Symposium on Telematics Applications*, pages 191–196.

[11] Ashuri, T., Reasnor, A. A. R. J. H. T., Ahmadi, S., and Iqbal, K. (2020). Biomedical soft robots:current status and perspective. *Biomedical Engineering Letters*.

[12] Berktay, H. O. (1983). *Resolution in Sonar Systems - A Review*. Springer.

[13] Bhushan, B. (2009). Biomimetics: lessons from nature-an overview. *Philosophical Transactions of the Royal Society*, 367:1445–1486.

[14] Bosselman, S. (2007). Electrical and mechanical behavior of silver-coated polymeric fibers. Technical report.

[15] Britton, A. C. and Jones, G. (1999). Echolocation behaviour and prey-capture success in foraging bats: Laboratory and field experiments on *Myotis daubentonii*. *The Journal of Experimental Biology*, 202(13):1793–1801.

[16] Brooks, R. A. (1986). A robust layered control system for a mobile robot. *IEEE Journal of Robotics and Automation*, 2(1):14–23.

[17] Caspers, P. (2017). *Analysis of Bat Biosonar Beampatterns: Biodiversity and Dynamics*. PhD thesis.

[18] Caspers, P. and Müller, R. (2015). Eigenbeam analysis of the diversity in bat biosonar beampatterns. *The Journal of the Acoustical Society of America*, 137(3):1081–1087.

[19] Chen, S., Pang, Y., Yuan, H., Tan, X., and Cao, C. (2020). Smart soft actuators and grippers enabled by self-powered tribo-skins. *Advanced Materials Technologies*, (1901075).

[20] Cho, K.-J., Koh, J.-S., Kim, S., Chu, W.-S., Hong, Y., and Ahn, S.-H. (2009). Review of manufacturing processes for soft biomimetic robots. *International Journal of Precision Engineering and Manufacturing*, 10(3).

[21] Cooke, J. R. (1988). Stepper motors: Principles and characteristics. *Proceedings of the Institution of Mechanical Engineers, Part D: Transport Engineering*, 202(2):111–117.

[22] Cornelia Geberl, K. K. and Wiegrebe, L. (2019). The spatial resolution of bat biosonar quantified with a visual-resolution paradigm. *Current Biology*, 29(11):1842–1846.

[23] Csorba, C., Ujhelyi, P., and Thomas, N. (2003). *Horseshoe Bats of the World*. Alana Books.

[24] Datteri, E., Teti, G., Laschi, C., Tamburrini, G., Dario, G., and Guglielmelli, E. (2003). Expected perception: an anticipation-based perception-action scheme in robots. In *Proceedings 2003 IEEE/RSJ International Conference on Intelligent Robots and Systems (IROS 2003)*, volume 1, pages 934–939. IEEE.

[25] Dehmollaian, M. and Sarabandi, K. (2006). Electromagnetic scattering from foliage camouflaged complex targets. *IEEE T Geosci Remote*, 44(10):2698–2709.

[26] Doppler, C. (1842). Über das farbige licht der doppelsterne und einiger anderer gestirne des himmels. *Abhandl Königl Böhm Gesellsch Wiss*, 2:465–482.

[27] Elgeneidy, K., Lohse, N., and Jackson, M. (2018). Bending angle prediction and control of soft pneumatic actuators with embedded flex sensors - a data-driven approach. *Mechatronics*, 50:234–247.

[28] Feng, L., Gao, L., and Müller, R. (2012). Noseleaf dynamics during pulse emission in horseshoe bats. *PLoS ONE*, 7(5):e34685.

[29] Fenton, M. B. (1990). The foraging behaviour and ecology of animal-eating bats. *Canadian Journal of Zoology*, 68:411–422.

[30] Fornshell, J. A. and Tesei, A. (2013). The development of sonar as a tool in marine biological research in the twentieth century. *International Journal of Oceanography*, 2013:678621.

[31] Freedman, A. (1962). A mechanism of acoustic echo formation. *Acta Acustica*, 12:10–21.

[32] Fu, Y., Caspers, P., and Müller, R. (2016). A dynamic ultrasonic emitter inspired by horseshoe bat noseleaves. *Bioinspiration and Biomimetics*, 11:036007.

[33] Gao, L., Balakrishnan, S., He, W., Yan, Z., and Müller, R. (2011). Ear deformations give bats a physical mechanism for fast adaptation of ultrasonic beam patterns. *Physical Review Letters*, 107:214301.

[34] Goebbel, L. (2002). Morphology of the external nose in hipposideros diadema and lavia frons with comments on its diversity and evolution among leaf-nosed microchiroptera. *Cells Tissues Organs*, 170(1):39–60.

[35] Gustafson, Y. and Schnitzler, H.-U. (1979). Echolocation and obstacle avoidance in the hipposiderid bat *Asellia tridens*. *J Comp Physiol*, 131(2):161–167.

[36] Han, J., A. Hsu, a. A. G., Cui, X., Audhaski, K., and M uller, R. (2018). Bioinspired dynamic frontend for spike-based speech recognition. *Neuro Inspired Computational Elements Workshop. Intel, Hillsboro, OR, February 2018*.

[37] Harris, F. J. (1978). On the use of windows for harmonic analysis with the discrete fourier transform. *Proceedings of the IEEE*, 66(1):51–83.

[38] He, W., Pedersen, S. C., Gupta, A. K., Simmons, J. A., and Müller, R. (2015a). Lancet dynamics in greater horseshoe bats,*Rhinolophus ferrumequinum*. *PLoS ONE*, 10(4):1–13.

[39] He, W., Pedersen, S. C., Gupta, A. K., Simmons, J. A., and Müller, R. (2015b). Lancet dynamics in greater horseshoe bats, rhinolophus ferrumequinum. *PLoS ONE*, 10(4):1–13.

[40] Hedrick, T. L. (2008). Software techniques for two- and three-dimensional kinematic measurements of biological and biomimetic systems. *Bioinspiration and Biomimetics*, 3(3).

[41] Hsu, A., Gupta, A., Müller, R., Cui, X., Audhkhaski, K., and Han, J.-P. (2017). Representations of speech signals recorded through a dynamic periphery inspired by horseshoe bat biosonar. *The Journal of the Acoustical Society of America*, 142:2706.

[42] Hu, W., Matlu, R., Li, W., and Alici, G. (2018). A structural optimisation method for a soft pneumatic actuator. *Robotics*, 7(2):24.

[43] Huang, X., Kumar, K., Jawed, M. K., Nasab, A. M., Ye, Z., Shan, W., and Majidi, C. (2018). Chasing biomimetic locomotion speeds: Creating untethered soft robots with shape memory alloy actuators. *Science Robotics*, 3(25).

[44] Javier Tapia, Espen Knoop, M. M., Otaduy, M. A., and Bächer, M. (2019). Makesense: Automated sensor design for proprioceptive soft robots. *Soft Robotics*.

[45] Jolliffe, I. (2002). *Principal Components Analysis, Second Edition*. Springer.

[46] Joseph, V. J., Gopi, S., and Subhadrabhai, D. (2013). Left-right resolution methods in towed arrays. *Ocean Electronics*.

[47] Kantorov, V. and Laptev, I. (2014). Efficient feature extraction, encoding and classification for action recognition. *Proceedings of the 2014 IEEE Conference on Computer Vision and Pattern Recoginition*, pages 2593–2600.

[48] Khyam, M. O., Alexandre, D., Bhardwaj, A., Wang, R., and Müller, R. (2019). Neuromorphic computing for autonomous mobility in natural environments. *Proceedings of ACM Conference(NICE Workshop), ACM, New York, NY, USA*.

[49] Kimura, K., Minami, R., Yamahama, Y., Takahiko, H., and Hosoda, N. (2020). Framework with cytoskeletal actin filaments forming insect footpad hairs inspires biomimetic adhesive device design. *Communications Biology*, 3(1):272.

[50] Klyubin, A. S., Polani, D., and Nehaniv, C. L. (2004). Organization of the information flow in the perception-action loop of evolved agents. In *Proceedings of the 2004 NASA/DoD Conference on Evolution Hardware*.

[51] Kobelev, Y. A. (2011). Multiple monopole scattering of sound waves from spherical particles in liquid and elastic media. *Acoustical Physics*, 57(6):749–7580.

[52] Kober, R. and Schnitzler, H.-U. (1990). Information in sonar echoes of fluttering insects available for echolocating bats. *The Journal of the Acoustical Society of America*, 87(2):882–896.

[53] Kuhn, G. F. (1987). *Physical Acoustics and Measurements Pertaining to Directional Hearing*, pages 3–25. Springer US, New York, NY.

[54] Linnenschmidt, M. and Wiegrebe, L. (2016). Sonar beam dynamics in leaf-nosed bats. *Science Reports-UK*, 6(29222).

[55] Lopez-Juarez, I. (2016). Skill acquisition for industrial robots:from stand-alone to distributed learning. In *2016 IEEE International Conference on Robotics and Automation*, pages 1–5.

[56] Ma, J. and Müller, R. (2011). A method for characterizing the biodiversity in bat pinnae as a basis for engineering analysis. *Bioinspiration and Biomimetics*, 6(026008).

[57] Marchese, A. D., Katzschmann, R. K., and Rus, D. (2015). A recipe for soft fluidic elastomer robots. *Soft Robotics*, 2(1):7–25.

[58] Meymand, S. Z., Pannala, M., and Müller, R. (2011). Characterization of dynamic baffles in biosonar and biomimetic devices. *The Journal of the Acoustical Society of America*, 130:2562.

[59] Ming, C., Gupta, A. K., Lu, R., Zhu, H., and Müller, R. (2017). A computational model for biosonar echoes from foliage. *PLoS ONE*, 12(8):e0182824.

[60] Mosadegh, B., Polygerinos, P., Keplinger, C., Wennstedt, S., Sheperd, R. F., Gupta, U., Shim, J., Bertoldi, K., Walsh, C. J., and Whitesides, G. M. (2014). Pneumatic networks for soft robotics that actuate rapidly. *Advanced Functional Materials*, 24(15):2163–2170.

[61] Moss, C. F. and Zagaeski, M. (1994). Acoustic information available to bats using frequency-modulated sounds for perception of insect prey. *The Journal of the Acoustical Society of America*, 95(5):2745–2756.

[62] Müller, R. (2010). Numerical analysis of biosonar beamforming mechanisms and strategies in bats. *The Journal of the Acoustical Society of America*, 128(3):1414–1425.

[63] Müller, R., Gupta, A., Zhu, H., Pannala, M., Gilani, U., Fu, Y., Caspers, P., and Buck, J. (2017). Dynamic substrate for the encoding sensory information in bat biosonar. *Physical Review Letters*, 118(15):158102 (5 pages).

[64] Müller, R., Gupta, A., Zhu, H., Pannala, M., Gillani, U. S., Fu, Y., Caspers, P., and Buck, J. R. (2017). Dynamic substrate for the physical encoding of sensory information in bat biosonar. *Physical Review Letters*, 118(15).

[65] Müller, R. and Kuc, R. (2000). Foliage echoes: A probe into the ecological acoustics of bat echolocation. *The Journal of the Acoustical Society of America*, 108(2):836–845.

[66] Müller, R. and Kuc, R. (2007). Biosonar-inspired technology: goals, challenges and insights. *Bioinspiration and Biomimetics*, 2(4):146–161.

[67] Müller, R., Sutlive, J., Caspers, P., and Fu, Y. (2016). A biomimetic perspective on the dynamics in horseshoe bat biosonar. *The Journal of the Acoustical Society of America*, 139(2115).

[68] Munich, A. (2010). ZVS Driver. https://adammunich.com/zvs-driver/.

[69] Neuweiler, G. (1989). Foraging ecology and audition in echolocating bats. *Trends in Ecology and Evolution*, 4(6):160–166.

[70] Neuweiler, G., Metzner, W., Heilmann, U., Rübsamen, R., Eckrich, M., and Costa, H. H. (1987). Foraging behaviour and echolocation in the rufous horseshoe bat (*Rhinolophus rouxi*) of sri lanka. *Behavioral Ecology and Sociobiology*, 20(1):53–67.

[71] Osborne, A. (1980). *An Introduction to Microcomputers*. Osborne/McGraw-Hill.

[72] Pailhas, Y., Petillot, Y., and Capus, C. (2010). High-resolution sonars: What resolution do we need for target recognition? *Eurasip Journal on Advances in Signal Processing*, (205095).

[73] Pannala, M., Ramakrishnan, N., and Müller, R. (2013). Dynamic encoding of sensory information in biomimetic sonar baffle. *The Journal of the Acoustical Society of America*, 134(5):4211.

[74] Paoletti, P., Jones, G., and Mahadevan, L. (2017). Grasping with a soft glove: intrinsic impedance control in pneumatic actuators. *Journal of the Royal Society Interface*, 14(128):20160867.

[75] Pillay, P. and Krishnan, R. (1991). Application characteristics of permanent magnet synchronous and brushless dc motors for servo drives. *IEEE Transactions on Industry Applications*, 27(5):986–996.

[76] Polygerinos, P., Lyne, S., Wang, Z., Nicolini, L. F., Mosadegh, B., Whitesides, G. M., and Walsh, C. J. (2013). Towards a soft pneumatic glove for hand rehabilitation. *IEEE/RSJ International Conference on Intelligent Robots and Systems*.

[77] Polygerinos, P., Wang, Z., Galloway, K. C., Wood, R. J., and Walsh, C. J. (2015). Soft robotic glove for combined assistance and at-home rehabilitation. *Robotics and Autonomous Systems*, 73:135–143.

[78] Pye, J. and Pye, A. (1962). Correlated orientation sounds and ear movements of horseshoe bats. *Nature*, 196:1186–1188.

[79] Qiu, P. and Müller, R. (2020). Variability in the rigid pinna motions of hipposiderid bats and their impact on sensory information encoding. *The Journal of the Acoustical Society of America*, 147(469).

[80] Regalia, G., Biffi, E., Ferrigno, G., and Pedrocchi, A. (2015). A low-noise, modular, and versatile analog fron-end intended for processing *In Vitro* neuronal signals detected by microelectrode arrays. *Computational Intelligence and Neuroscience*, page 172396.

[81] Riopelle, N., Caspers, P., and Sofge, D. (2018). Terrain classification for autonomous vehicles using bat-inspired echolocation. In *2018 International Joint Conference on Neural Networks (IJCNN)*, pages 1–6.

[82] Runciman, M., Darzi, A., and Mylonas, G. P. (2019). Soft robotics in minimally invasive surgery. *Soft Robotics*, 6(4):423–443.

[83] Rus, D. and Tolley, M. T. (2015). Design, fabrication, and control of soft robots. *Nature*, 521:467–475.

[84] Sailant, P., Simmons, J., Dear, S., and McMullen, T. (1993). A computational model

of echo processing and acoustic imaging in frequency-modulated echolocating bats. *The Journal of the Acoustical Society of America*, 94(5):2691–2712.

[85] Samant, S., Sabuwala, M. H., Gokalgandhi, B., and Pandey, A. (2014). Plasma speaker. *International Journal of Scientific Engineering Research*, 5(9).

[86] Scaramuzza, D., Achtelik, M. C., Doitsidis, L., Friedrich, F., Kosmatopoulos, E., Martinelli, A., Achtelik, M. W., Chli, M., Chatzichristofis, S., Kneip, L., Gurdan, D., Heng, L., Lee, G. H., Lynen, S., Pollefeys, M., Renzaglia, A., Siegwart, R., Stumpf, J. C., Tanskanen, P., Troiani, C., Weiss, S., and Meier, L. (2014). Vision-controlled micro flying robots: From system design to autonomous navigation and mapping in gps-denied environments. *IEEE Robotics and Automation Magazine*, 21(3):26–40.

[87] Schneider, H. and Möhres, F. P. (1960). Die ohrbewegungen der hufeisenfledermäuse (chiroptera, rhinolophidae) und der mechanismus des bildhörens. *Journal of Comparative Physiology*, 44:1–40.

[88] Schnitzler, H.-U., Moss, C. F., and Denzinger, A. (2003). From spatial orientation to food acquisition in echolocating bats. *Trends in Ecology and Evolution*, 18(8):386–394.

[89] Schoeppler, D., Schnitzler, H.-U., and Denzinger, A. (2018). Precise doppler shift compensation in the hipposiderid bat, *Hipposideros armiger*. *Scientifc Reports*, 8:4598.

[90] Shepard, R. F., Ilievski, F., Choi, W., Morin, S. A., Stokes, A. A., Mazzeo, A. D., and Whitesides, G. M. (2011). Multigait soft robot. *Proceedings of the National Academy of Sciences of the United States of America*, 108(51):20400–20403.

[91] Shieldex-US (2020). Yarns/threads. https://www.shieldextrading.net/products/yarns-threads/. accessed: 06-18-2020.

[92] Silva, A. (2009). Optimized litz wire. U.S. patent no. 20090295531.

[93] Simmons, J. A. (1971). Echolocation in bats:signal processing of echoes for target range. *Science*, (3974):925–928.

[94] Simmons, N. (2005). Order chiroptera. In Reeder, D., editor, *Mammal Species of the World: A Taxonomic and Geographic Reference*. Johns Hopkins University Press.

[95] Smotherman, M. and Guillén-Servent, A. (2008). Doppler-shift compensation by wagner's mustached bat,*Pteronotus personatus*. *The Journal of the Acoustical Society of America*, 123(6):4331–4339.

[96] Song, K., Kim, S. H., Jin, S., Kim, S., Lee, S., Kim, J.-S., Park, J.-M., and Cha, Y. (2019). Pneumatic actuator and flexible piezoelectric sensor for soft virtual reality glove system. *Scientific Reports*, 9:8988.

[97] Streelman, J. and D.Danley, P. (2003). The stages of vertebrate evolutionary radiation. *Trends in Ecology and Evolution*, 18:126–131.

[98] Suga, N., Neuweiler, G., and Möller, J. (1976). Peripheral auditory tuning for fine frequency analysis by the cf-fm bat, *Rhinolophus ferrumequinum*. *Journal of Comparative Physiology*, (106):111–125.

[99] Sullivan, K., Conk, M., Eckman, E., Lunsford, S., Martin, C., Singh, A., Wang, Y., Sutlive, J., and Müller, R. (2019). Design and manufacturing of a miniature pneumatic actuator for a bat robot. *Journal of the Acoustical Society of America*, 45(171).

[100] Sutlive, J. and Müller, R. (2019). Dynamic echo signatures created by a biomimetic sonar head. *Bioinspiration and Biomimetics*, 14(6):066014.

[101] Sutlive, J., Singh, A., Zhang, S., and Müller, R. (2020). A biomimetic soft robotic pinna for emulating dynamicreception behavior of horseshoe bats. *Bioinspiration and Biomimetics*.

[102] Todd, B. D. (2017). Comparison of the role of beamwidth in biological and engineered sonar. Master's thesis.

[103] Touchette, H. and Lloyd, S. (2004). Information-theoretic approach to the study of control systems. *Physica A*, 331(1-2):140–172.

[104] Trevorrow, M. (2002). High frequency acoustic scattering and absorption effects in ship wakes. Technical report.

[105] Trivedi, D., Rahn, C. D., Kierb, W. M., and Walker, I. D. (2008). Soft robotics: Biological inspiration, state of the art, and future research. *Applied Bionics and Biomechanics*, 5(3):99–117.

[106] Truby, R. L. and Lewis, J. A. (2016). Printing soft matter in three dimensions. *Nature*, 540:371–378.

[107] Trzynadlowski, A. M. (2010). *Introduction to Modern Power Electronics*. Wiley.

[108] Urick, R. and Pryce, A. (1953). A summary of underwater acoustic data, part ii: Target strength.

[109] Vincent, J. F. V. (2009). Biomimetics–a review. *Proceedings of the Institution of Mechanical Engineers, Part H*, 23(8):919–939.

[110] Von der Emde, G. and Menne, D. (1989). Discrimination of the insect wingbeat-frequencies by the bat *Rhinolophus ferrumequinum*. *Journal of Comparative Physiology A*, 164(5):663–671.

[111] Waite, A. (2002). *Sonar for Practising Engineers*. Wiley, 3rd edition edition.

[112] Wang, H., Totaro, M., and Beccai, L. (2018). Toward perceptive soft robots: Progress and challenges. *Adv Sci (Weinh)*, 5(9):1800541.

[113] Washington, S. D. and Kanwall, J. S. (2008). Dscf neurons within the primary auditory cortex of the mustached bat process frequency modulations present within social calls. *Journal of Neurophysiology*, 100(6).

[114] Wehner, M., Truby, R. L., Fitzgerald, D. J., Mosadegh, B., Whitesides, G. M., Lewis, J. A., and Wood, R. J. (2016). An integrated design and fabrication strategy for entirely soft, autonomous robots. *Nature*, 536:451–455.

[115] Wilson, D. and Reeder, D. M. (2005). *Mammal species of the world: A taxonomic and geographic reference*, volume 1. Johns Hopkins University Press.

[116] Yang, G.-Z., Bellingham, J., Dupont, P. E., Fischer, P., Floridi, L., Full, R., Jacobstein, N., Kumar, V., McNutt, M., Merrifield, R., Nelson, B. J., Scassellati, B., Taddeo, M., Taylor, R., Veloso, M., Wang, Z. L., and Wood, R. (2018a). The grand challenges of *Science Robotics*. *Science Robotics*, 3(eaar7650).

[117] Yang, L., Yu, A., and Müller, R. (2018b). Design of a dynamic sonar emitter inspired by hipposiderid bats. *Bioinspiration and Biomimetics*, 13(5):056003.

[118] Yang, X., Chang, L., and Pérez-Arancibia, N. O. (2020). An 88-milligram insect-scale autonomous crawling robot driven by a catalytic artificial muscle. *Science Robotics*, 5(45).

[119] Yin, X. and Müller, R. (2017). Quantification of fast pinna motions in rhinolophid and hipposiderid bats. *The Journal of the Acoustical Society of America*, 142:2664.

[120] Yin, X. and Müller, R. (2019). Fast-moving bat ears create informative doppler shifts. *Proceedings of the National Academy of Sciences of the United States of America*, 116(25):12270–12274.

[121] Yin, X., Qiu, P., Zhang, M., and Müller, R. (2016). Quantitative analysis of rigid

and non-rigid motion patterns in rhinolophid and hipposiderid pinnae. *Journal of the Acoustical Society of America*, 140:2974–2974.

[122] Yong-Nong, C. and Chih-Ming, K. (2013). Design of a plasma generator driven by a high-frequency, high-voltage power supply. *Journal of Applied Research and Technology*, 11(2).

[123] Zhang, L., Bhardwaj, A., and Müller, R. (2019a). Deep learning of biosonar landmarks for navigation in forest environments. *J. Acoust. Soc. Am.*, 146(4):3025.

[124] Zhang, L. and Müller, R. (2020). An experimental link between fast noseleaf deformation and biosonar pulse dynamics in hipposiderid bats. *J. Acoust. Soc. Am.*, 148(2):954–961.

[125] Zhang, S., Liu, Y., Tang, J., Ying, L., and Müller, R. (2019b). Dynamic relationship between noseleaf and pinnae in echolocating hipposiderid bats. *The Journal of Experimental Biology*, 222:jeb.210252.

[126] Zhao, J. and Abbas, A. (2016). A low-cost coiled sensor for soft robots. *ASME 2016 Dynamic Systems and Control Conference*, 2.

Appendices

Appendix A

Sonar head version 4 design

This appendix describes the design paradigms of the fourth version of the sonar head, which was used to collect the data illustrating dynamic signatures present in echoes. This sonar head has been used to collect data described in [48, 100].

A.1 Mechanical Design

The design of the fourth sonar head allowed for it to be mounted to various devices through slits in the top and bottom as well as hand-carried to collect data (design shown in 1.2). The sonar head frame was constructed of acrylic for non-load-bearing elements and polyoxymethtlene (delrin) for primary load support. The electronics were housed in a compartment in the rear of the sonar head, while all the sonar elements were mounted to a trapezoidal structure on the front of the sonar head. A total of five stepper motors were used to actuate the ears and noseleaf of the sonar head. Two larger (NEMA 17) stepper motors were responsible for the pinna actuation, while two smaller (NEMA 11) motors actuated opposite sides of the anterior leaf. A waveguide was used to direct sound from two electrostatic speakers (Senscomp, Livonia, Michigan) and to help create an approximation of a point source. This allows the sound to illuminate the noseleaf, resulting conformation changes/ rapid deformations of the noseleaf affecting the outgoing sound. To help guide decision-making regarding ear position on the sonar head, a beampattern was taken of the pinna baffle and micophone.

The beampattern indicated that the pinna was more responsive to sound above it compared to sounds directly in front of it or below, as it was more responsive to sounds towards the center of the sonar than to the sides. With these properties in mind, the ears were angled 15°downwards (along x-axis, where x represents the width of the sonar head) and 10°towards the sides (along z-axis, where z represents the height of the sonar head). This helped align the beampatterns of the emitter and receiver.

A.2 Electronics

The electronics of this system (see figure A.1) were altered from previous versions to support the sonar head functioning as a portable system. There is a single board which acts as both amplifier and power distribution board. A two-stage AB-type amplifier drives two electrostatic speakers responsible for creating the pulses emitted from the amplifier. The power supply unit uses a small ATX power supply (Pico PSU, Ituner Networks Corporation, Fremont, California) to power the system. An additional boost converter is used to generate the high voltage (400V at .1A) required to drive the power amplifier of the emission system. Additionally, a shield over the motor controller is responsible for driving the stepper motors.

A.3 Software

The sonar head uses a SAM3X-based microcontroller (Arduino Due, Arduino, Ivrea Italy) to handle data acquisition, an ATMega-based microcontroller for motion control (Arduino Mega, Arduino, Ivrea, Italy), and an ARM-based single board computer to act as an onboard computer which starts and stops the system and provides the user interface (Raspberry Pi

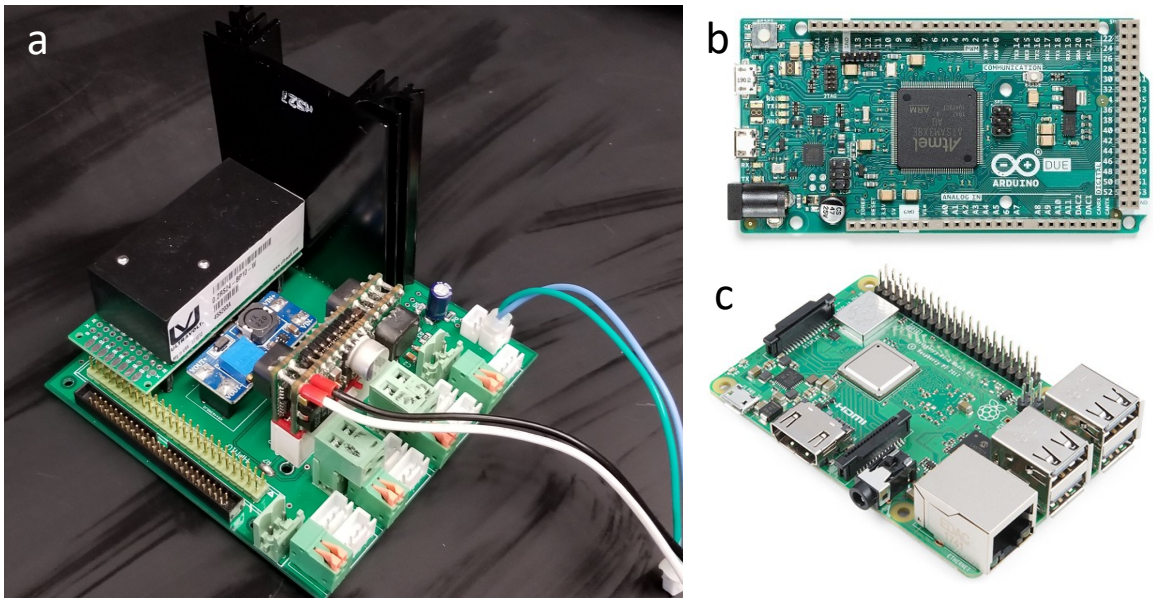

Figure A.1: **Electronics/ microcontrollers used on sonar head 4:**a. Integrated power distribution and amplifier board. b. Arduino Due microcontroller for data acquisition. c. Raspberry Pi single-board computer for user interface and/or data storage. Not pictured: Arduino Mega motor controller/ motor driver shield.

3, Adafruit, New York, NY). The interface was designed to run in "headless" mode, i.e. the system would collect data without input from the user whenever it was powered on. For in-lab experiments, the system could be configured to use a monitor. A small monitor was later added to the device, though there was not enough power to operate the entire system at maximum efficiency, thus any plotting/monitoring software ran very slow (1 echo per 10 seconds) in this version of the system.

Appendix B

Sonar head version 5 design

This appendix describes the design paradigms of the fifth version of the sonar head, currently in construction (see figure 3.1b for a rendering of the design in progress). The ear system of this model was used to show the effects of different motion profiles on acoustic data and is the first to include the base components for a motor feedback system. As the design is currently in its final stages of completion, there may be some discrepancies between what is described here and the final product. An incomplete prototype version of this sonar head was used to collect data in [101].

B.1 Mechanical Design

The sonar head used carbon fibre for load-bearing components and acrylic for non-load-bearing elements. Added to this version of the sonar head will be a touchscreen interface, as well as cameras to provide a stereo image. The overall size of the system is slightly larger to accommodate the additional systems inside the sonar head. There are two sets of mounts which protrude vertical in opposite directions from the sonar head; these are to allow mounting to a pan-tilt, zip-line, or drone platform for laboratory or field experiments.

The new design of the sonar head uses updated versions of the pinna and noseleaf. These are actuated with a pneumatic actuation system using a system of 16 valves (see chapter 3 for details). Additionally, a pan-tilt system has been designed to replicate the rigid ear rotations

seen in horseshoe bats [79].

Inside the sonar head, the electronics are elevated off the floor of the sonar head to allow for improved cable management and easier access to devices when debugging. The programming ports of all microcontrollers as well as USB, ethernet, and HDMI interfaces from the Jetson are available to the user from the outside of the box on the side panels.

B.2 Electronics

The electronics of the system have been updated from the previous version. This was to keep the system up-to-date as well as fix issues present on the previous system. As in the previous robot design, the main systems of the robot are:

- Power system
- Emitter/ amplifier system
- Motor control systems

The power system on the robot was updated to allow each individual line to be able to draw significantly more power. To accomplish this, the design was updated with modular power converters. The design uses switching converters, which are currently the most efficient method of power conversion [107] each rated at 40 W.This is to ensure all components have enough power to run efficiently. This specifically fixes issues with the onboard computer system in the last build, which did not receive enough power to remain stable, especially if an external monitor was attached. The design is modular, with each card being able to "plug in" to a slot on a power hub within the sonar head, with the cards being removable from the outside. This allows the user to be able to alter the power system of the sonar head

should power requirements change.

Problems with the previous sonar head's emission system resulted in the experimentation with different emission system designs. The device needs an emission system which can produce an omnidirectional source to illuminate the noseleaf while also producing an adequate output signal to be able to maximize signal-to-noise level in the system. Conventional speakers often are very directional and can create distortions if trying to produce frequencies outside their ideal frequency band [85]. To address these issues a plasma tweeter was designed. This is a unique tweeter design in which sound is created by modulating an arc of electricity over a short distance [85, 122]. This is essentially accomplished by designing a high voltage power supply where the switching frequency driving the supply can be adjusted using a microcontroller [68]. Modern high-voltage power supply designs are resonant converters, which use the properties of electrical resonance coupled with those of an inductor-capacitor (LC) tank to generate high voltages with limited switching losses [107]. The tweeter functions as follows: an input waveform (desired audio) drives the gate of either one or two MOSFETs, which convert that voltage to a square wave. Resonance across the switch produces a sinusoidal waveform at the switch output [107]. A resonant circuit (LC tank) connected to this, then provides the step-up needed, creating a high-voltage sinusoid with the same frequency the MOSFET is switching at, which in turn is being controlled by our input waveform. While in a normal converter circuit, a rectifier would be used to convert the AC signal to a DC one [107], the tweeter simply arcs this high voltage signal over a small gap [68]. This results in the air becoming ionized, resulting in a massless speaker that produces sound over a plasma arc [85]. An updated version of the tweeter was designed using a different flyback transformer which would alter the resonance peak, pushing it to 120 kHz (original and updated designs depicted in figure In preliminary testing, the device has been able to emit a high frequency sound with little interference from the LC tank resonance with

use of the updated flyback transformer. The system should be backwards compatible, so if

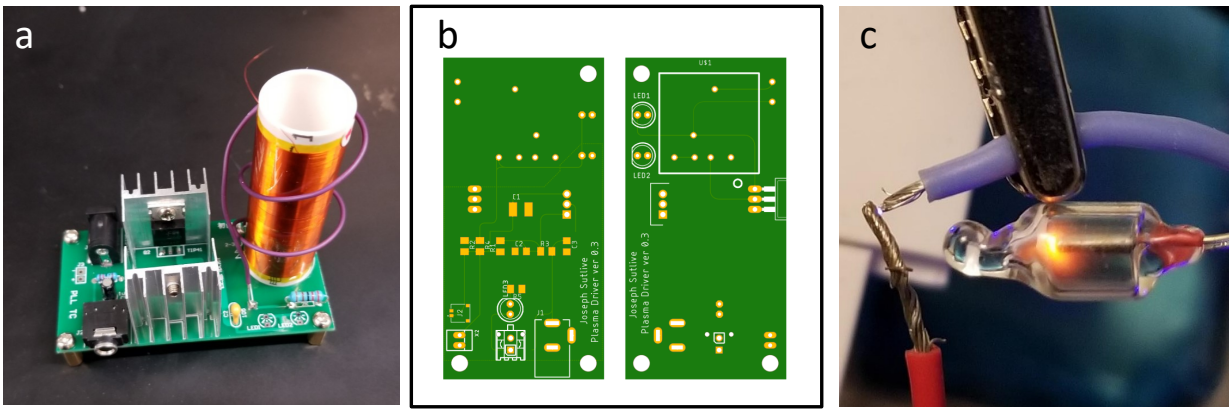

Figure B.1: **Plasma tweeter intial and updated designs:**a. Original model of a plasma tweeter, purchased online as a "singing tesla coil", and used as a reference for future circuits. b. Updated circuit for the plasma tweeter's driving circuit c. A small (<3mm) gap is produced by the revised version of the plasma tweeter. Electromagnetic interference causes the halogen bulb to glow.

this design has problems with implementation, reverting to the previous amplifier system should not be difficult.

The motor control systems consist of driver circuitry designed to take low-power control signals from a microcontroller and drive the motors and valves for the sonar head. A series of MOSFETs are used to drive the valves, while specialized driver circuits are used to drive two stepper motors. Servos need no additional driver circuitry (the driver is onboard)

B.3 Software

This sonar head featured the addition and expansion of the software system on the sonar head. As this design added more motor functionality when compared with the previous system (16 valves/4motors compared with 5 motors), the motor control is handled by two devices separately to account for this. The devices are organized by the devices they control,

motors are driven using one device, valves with the other (two Teensy 4.0, PJRC, Sherwood, Oregon). The data acquisition system uses an improved chipset (SAMD51) compared with the previous version (SAM3X), integrated on a new microcontroller (M4 Grand Central, Adafruit, New York, New York). This system upgraded the method of data acquisition and transfer to using direct memory access (DMA), which by using a controller (DMAC), can initiate memory read/write cycles independently of the CPU [71].

Finally, the onboard computer was upgraded to include more powerful specifications (Jetson Nano, Nvidia, Santa Clara, California). This new system featured a separate graphics chipset (128-core Maxwell), as well as significantly more RAM (4 GB). Additionally, by using NVIDIA's JetPack API, the user has the ability to integrate algorithms optimized to run on the Jetson hardware, allowing for further expansion of the system capabilities. The new system uses a GUI to allow the user to be able to interface easily with the sonar head and to actively monitor echoes as they return to the system, utilizing a small touchscreen monitor mounted to the rear of the sonar head. It has shown to be more responsive than the previous version of the sonar head in its current state.

The low-level controllers (motion and data acquisition) communicate to each other via serial peripheral interface (SPI). The onboard computer communicates with the data acquisition unit via a Universal Asynchronous Receiver/Transmitter (UART) protocol. Due to the nature of the system and the need to acquire date on a millisecond timescale, the latency between systems must be as low as possible, particularly between systems performing tasks during or for data acquisition. These protocols were determined to be the optimal method of transmission given the low latency produced.